Please cite this article in press as: Takahashi et al., *ERBB4* Mutations that Disrupt the Neuregulin-ErbB4 Pathway Cause Amyotrophic Lateral Sclerosis Type 19, The American Journal of Human Genetics (2013), http://dx.doi.org/10.1016/j.ajhg.2013.09.008

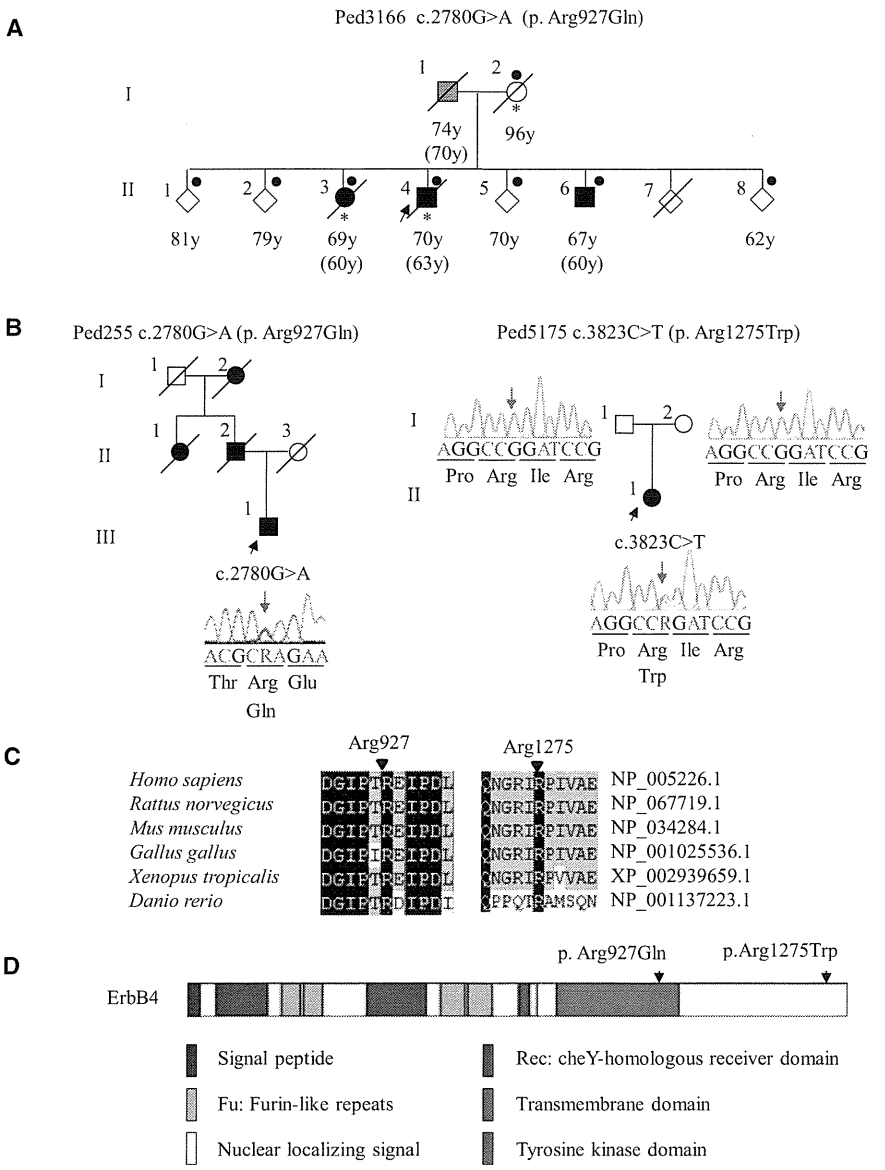

Figure 1. Pedigrees of ALS and Characterization of Mutations

(A) Pedigree charts of the index family. Filled symbols indicate affected individuals. The arrow indicates the proband. For confidentiality purposes, all unaffected siblings are indicated by diamonds. Dots or asterisks indicate individuals included in the linkage study or WGS, respectively. Age at present or age at death is shown under each individual, and ages at onset are shown in parentheses. The box with gray shading indicates that the individual's clinical information obtained from the family members strongly supports the diagnosis of ALS, although detailed neurological evaluations have not been conducted for this individual.

(B) Additional Canadian (Ped255) and Japanese (Ped5175) pedigrees with *ERBB4* mutations. The electropherograms of mutational data are shown beside each member. Nucleotide colors correspond to the colors in the electropherograms. The amino acids are designated below the nucleotide sequences. The blue arrows indicate the nucleotide positions of the mutations. In the electropherograms (Ped5175), nucleotide sequences of the reverse complementary strand are shown.

(C) Amino acid conservation. The amino acids Arg927 and Arg1275 are highly conserved among species.

(D) The protein structure along with the locations of amino acid substitutions are shown; amino acid substitutions are indicated by arrows. The amino acid substitution p. Arg927Gln resides in the tyrosine kinase domain, which mediates the key functions of ErbB4. The amino acid substitution p. Arg1275Trp resides in the C-terminal domain in the vicinity of multiple phosphorylation sites, which mediate downstream signaling pathways.

sequencing technologies has allowed us to overcome the difficulty by means of whole-genome sequencing (WGS) or exome analysis.

We identified a Japanese family with three affected siblings presenting with late-onset ALS (Figure 1A and Table 1). The familial history indicated that the mode of inheritance is probably an autosomal-dominant one. Mutational analysis of the proband (II-4) employing direct nucleotide sequence analysis, a microarray-based resequencing, or a repeat-primed PCR analysis excluded *SOD1*[MIM 147450], *ALS2*[MIM 606352], *DCTN1*[MIM 601143], *CHMP2B*[MIM 609512], *ANG*[MIM 105850], *TARDBP*[MIM 605078], *FUS*[MIM 137070] and *C9ORF72* [MIM 1614260] as the genes associated with FALS.[3,4] To identify a gene associated with FALS, we applied WGS in combination with a linkage analysis to the pedigree. Written informed consent was obtained from all the participants. This study was approved by the institutional review board at the University of Tokyo.

WGS was performed on three individuals (I-2, II-3 and II-4, as shown in Figure 1A) in the index pedigree. Paired-end DNA libraries were generated and subjected to massively parallel sequencing with a GAII Illumina Genome Analyzer in accordance with the manufacturer's instructions. The short read sequences obtained were aligned to the reference genome (NCBI37/hg19 assembly) via the Burrows-Wheeler Aligner.[5] Downstream analyses in which potential PCR duplicates were removed were processed with SAMtools.[6] Aligned reads were viewed on an Integrative Genomics Viewer.[7] Genomic sequence variations were identified with the SAMtools pileup command and annotated with Refseq, dbSNP135, 1000 Genomes, personal genome databases, the NHLBI GO Exome Sequencing Project (NHLBI-ESP) database, and an in-house variant database containing 41 whole genomes and 1,408 exomes in the Japanese population. The numbers of nonsynonymous variants that were identified in individuals I-2, II-3, and II-4 but that were not present in any of the

Please cite this article in press as: Takahashi et al., *ERBB4* Mutations that Disrupt the Neuregulin-ErbB4 Pathway Cause Amyotrophic Lateral Sclerosis Type 19, The American Journal of Human Genetics (2013), http://dx.doi.org/10.1016/j.ajhg.2013.09.008

Table 1. Clinical Characteristics of Affected Individuals

Pedigree Number	Pedigree 3166				Pedigree 255	Pedigree 5175
Ethnicity	Japanese				Canadian	Japanese
Inheritance	familial (autosomal dominant)				familial (autosomal dominant)	simplex
Mutation	c.2780G>A				c.2780G>A	c.3823C>T
Amino acid substitution	p. Arg927Gln				p. Arg927Gln	p. Arg1275Trp
Members	I-1	II-3	II-4 (proband)	II-6	III-3	II-1
Age at onset	70	60	63	60	67	45
Initial symptoms	bulbar	N.D.	upper limbs	respiration	upper limbs	upper limbs
Diagnostic criteria[a]	N.D.	N.D.	definite	definite	probable	probable
Progression	unable to walk after 3 years	ventilator -dependent after 5 years, locked-in state after 8 years	locked-in state after 5 years	ventilator- dependent after 1 year, locked-in state after 5 years	slow progression that significantly decelerated and finally stopped after 8 years	wheelchair- bound, MRS 1-2/5 in upper extremities after 5 years
Cognitive function	N.D.	N.D.	normal	normal	N.D.	normal
Age at death	74	69	70	66	N/A	N/A

Abbreviations are as follows: N.D., not described; MRS, manual muscle testing rating scale; and N/A, not applicable.
[a]El Escorial and Airlie House revised criteria.

databases (hereafter, variants not found in the databases are referred to as "novel") were 411, 404, and 382, respectively (Table S1). No novel nonsynonymous variants in genes known to be associated with FALS were included. Among the identified variants, 57 were identified both in the proband and in the affected sibling, but not in the mother, and were subjected to further analysis.

The individuals indicated by dots in Figure 1A were genotyped with Genome-Wide Human SNP Array 6.0 (Affymetrix). Linkage analysis and haplotype reconstruction were conducted with the pipeline software SNP-HiTLink[8] and Allegro version 2[9] under the assumption of an autosomal-dominant mode of inheritance and a disease-allele frequency of 0.000001. Parametric multipoint linkage analysis under the assumption of complete penetrance revealed three loci spanning 23.6 Mb on chromosomes 1, 6, and 13, having a maximum LOD score of 1.8 (Figure S1; penetrance = 1.0), and containing 88 annotated genes. However, no novel nonsynonymous variants were identified in the candidate regions. We then considered the possibility of reduced penetrance. When penetrance was reduced to 0.8 (Figure S1), seven additional loci had LOD scores > 0.7 and were thus shown to support linkage; these loci contained 809 annotated genes. Three heterozygous novel nonsynonymous variants were identified in these regions; among these variants, only c.2780G>A (p. Arg927Gln; dbSNP SubSNP ID ss831884245) substituting glutamine for arginine at codon 927 (p. Arg927Gln) in v-erb-a erythroblastic leukemia viral oncogene homolog 4 (avian) (*ERBB4* [MIM 600543; RefSeq accession number NM_005235.2]) was not present in 477 controls (Table S2). When we allowed further reduced penetrance, we identified 19 additional loci with LOD > 0; these loci contained 1,265 annotated genes. In these regions, we identified seven heterozygous novel nonsynonymous variants, among which three variants in *OR2D3* (RefSeq NM_001004684.1), *FTCD* (MIM 606806; RefSeq NM_206965.1), and *TJP2* (MIM 607709; RefSeq NM_001170414.2) were not present in 477 controls (Table S2). *OR2D3* is an olfactory receptor gene; the substituted amino acid in *OR2D3* is not conserved, and the substitution is predicted as benign by PolyPhen-2 analysis. *FTCD* and *TJP2* are associated with autosomal-recessive glutamate formiminotransferase deficiency (MIM 229100) and familial hypercholanemia (MIM 607748), respectively, and heterozygous carriers have not been described as exhibiting ALS. Taken together, the results pointed to c.2780G>A in *ERBB4* as the most likely pathogenic mutation.

We used a direct nucleotide sequence analysis method to conduct mutational analysis of *ERBB4* in 364 FALS and 818 SALS individuals by using an ABI 3100 sequencer and BigDye Terminator ver3.1 (Applied Biosystems). We used the ExonPrimer website to design oligonucleotide primers (Table S3). The mutation c.2780G>A was also identified in one Canadian FALS individual (Figure 1B). Unfortunately, DNA from other family members was not available to confirm segregation. To investigate a possibility that the c.2780G>A mutation identified in the Japanese and Canadian families is a common founder mutation, we compared the haplotypes with the c.2780G>A mutation in *ERBB4* of the Japanese and Canadian families (Figure S2). Different SNPs were observed 14 kbp and 5 kbp centromeric and telomeric to the mutation, respectively, indicating that disease haplotypes of the Japanese and Canadian families are different and that

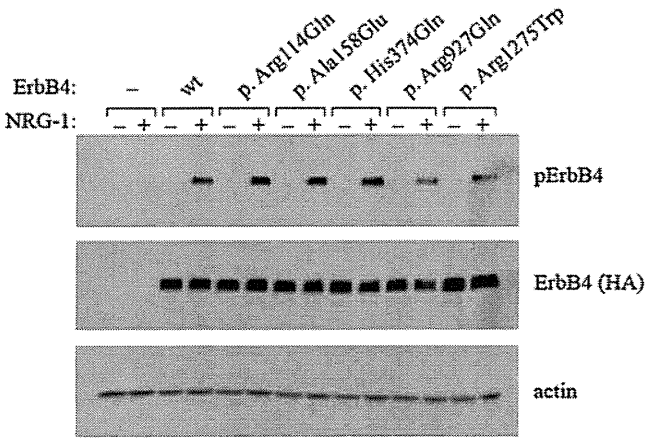

Figure 2. Functional Analysis of Wild-Type and Mutant ErbB4 upon Neuregulin-1 Stimulation

COS-7 cells transfected with an empty-vector control or plasmids encoding either wild-type (wt) or mutant HA-tagged ErbB4 (p. Arg114Gln, p. Ala158Glu, p. His374Gln, p. Arg927Gln, or p. Arg1275Trp) were stimulated with or without NRG-1, and the autophosphorylation activity of ErbB4 was analyzed by immunoblot analysis with antibodies against phospho-ErbB4 (Tyr1284) (Cell Signaling) and HA tag (Abcam), respectively. For loading controls, immunoblotting was performed with an anti-actin antibody (Santa Cruz Biotechnology). Three amino acid substitutions, including p.Arg114Gln, p.Ala158Glu, and p.His374Gln (rs760369), identified through mutational analysis of FALS and SALS individuals, were included in autophosphorylation assay. The substitutions p.Arg114Gln and p.Ala158Glu were not considered to be relevant to ALS because neither recurrence nor cosegregation was confirmed.

mutation occurred independently. We identified a de novo mutation of c.3823C>T (dbSNP SubSNP ID ss831884246), substituting tryptophan for arginine at codon 1275 (p. Arg1275Trp), in a Japanese SALS individual (Figure 1B) in whom a biological parent-descendant relationship was confirmed (Table S4) by the PLINK[10] algorithm. These mutations were neither present in the 477 Japanese controls nor registered in the in-house database containing 41 whole genomes and 1408 exomes, the 1000 Genomes database, or the NHLBI-ESP database, containing 6503 exomes. Furthermore, c.2780G>A was not present in 190 Canadian controls. The identification of c.2780G>A in two independent families of different ethnic backgrounds strongly supported c.2780G>A as the causative mutation for ALS. Given that de novo mutation rates have been estimated to be 1.20×10^{-8} per nucleotide per generation[11] and less than one nonsynonymous single-nucleotide variant (SNV)/generation,[12] the observation of the de novo mutation further supports the idea that c.3823C>T is likely to be the causative mutation for ALS in this individual. The mutation's substituted arginine residues, Arg927 and Arg1275, are highly conserved among species (Figure 1C), and the substitutions are predicted to be probably damaging by PolyPhen-2 analysis. The amino acid residue Arg927 resides in a tyrosine kinase domain, which is essential for the receptor tyrosine kinase activity, and Arg1275 is located in a C-terminal domain in the vicinity of multiple phosphorylation sites, which mediate downstream signaling pathways (Figure 1D). The clinical presentations of these ALS individuals with the *ERBB4* mutations are summarized in Table 1. The common clinical characteristics of the individuals included both upper and lower motor-neuron involvement diagnosed as definite or probable ALS according to El Escorial and Airlie House revised criteria, relatively slow disease progression, and no obvious cognitive impairment. The individuals with the c.2780G>A mutation were characterized by relatively late onset (the ages at onset ranged from 60–70 years) and a slightly reduced penetrance. In contrast, the individual with the c.3823C>T mutation was characterized by early onset (45 years of age).

ErbB4 is a member of the epidermal growth factor (EGF) subfamily of receptor tyrosine kinases (RTKs). It forms a homodimer or a heterodimer with ErbB2 or ErbB3 and is activated upon binding of neuregulins (NRGs) to the extracellular ligand-binding domain of ErbB4.[13] Activation of ErbB4 is mediated by increased tyrosine kinase activity upon NRG binding, resulting in autophosphorylation of the C-terminal tail.[14] To determine how the two mutations identified in the ALS individuals affect ErbB4 functions, we investigated the autophosphorylation of ErbB4 in cells expressing either wild-type or mutant (c.2780G>A or c.3823C>T) *ERBB4* in the presence of NRG-1. The *ERBB4* mutations were introduced into the pBABE-puro*ERBB4JM-aCYT-2HA* plasmid encoding HA-tagged ErbB4 JM-a CYT-2[15] by site-directed mutagenesis according to the protocol described in the Phusion Site-Directed Mutagenesis Kit (Thermo Fisher Scientific). After mutagenesis, all the constructs were verified by sequencing. The plasmids were transiently transfected into COS-7 cells via FuGENE 6 transfection reagent (Roche) in accordance with the manufacturer's instructions. Transfected cells were starved of serum overnight and stimulated with 0 or 50 ng/ml NRG-1 (R&D Systems) for 10 min at 37°C. After stimulation, the cells were lysed, and samples equivalent to 50 μg of total protein were separated through 8% SDS-PAGE gels. For detectiin of ErbB4 phosphorylation and total ErbB4 protein levels, immunoblotting was performed antibodies against phospho-ErbB4 (Tyr1284) (Cell Signaling) and HA-tag (Abcam), respectively. The two amino acid substitutions, p. Arg927Gln and p. Arg1275Trp, showed a clearly reduced autophosphorylation of ErbB4 (Figure 2). On the basis of these genetic and functional data, we concluded that the two mutations are causative mutations for ALS (ALS19).

This study revealed that a reduced autophosphorylation of ErbB4 upon NRG-1 stimulation is involved in the pathogenesis of ALS. *Erbb4* is specifically expressed in the soma of large motor neurons of the rat spinal cord.[16] The lack of *Erbb4* is embryonically lethal in mice, which displayed the derangement of motor-neuron axon guidance and pathfinding during embryogenesis.[17] Heterozygous-null mice showed a reduced body weight and delayed motor development, and brain-specific conditional knock-out mice

demonstrated reduced spontaneous motor activity and grip strength of the hindlimbs.[18] Mice lacking cysteine-rich domain (CRD) isoforms of *Nrg-1* (*CRD-NRG-1*$^{-/-}$) die perinatally as a result of respiratory failure, lack detectable limb movement, and exhibit a loss of ~60% of spinal motor neurons.[19] Similarly, motor and sensory neuron-specific conditional *Nrg-1* knockout mice die at birth and showed marked retraction of motor-neuron axons.[20] Furthermore, a decrease in the amount of CRD-NRG-1 has been detected in the spinal motor neurons in FALS and SALS individuals and *Sod1* mutant mice at disease onset,[21] raising the possibility that disruption of the NRG-ErbB pathway is commonly involved in the motor-neuron degeneration underlying ALS. This study provides insight into ALS pathogenesis and is expected to pave the way for the development of innovative therapeutic strategies such as using NRGs or their agonists to upregulate ErbB4 functions.

Supplemental Data

Supplemental Data include two figures and four tables and can be found with this article online at http://www.cell.com/AJHG/.

Consortia

Consortium members of JaCALS include Ryoichi Nakamura, Hazuki Watanabe, Yuishin Izumi, Ryuji Kaji, Mitsuya Morita, Kotaro Ogaki, Akira Taniguchi, Ikuko Aiba, Koichi Mizoguchi, Koichi Okamoto, Kazuko Hasegawa, Masashi Aoki, Akihiro Kawata, Imaharu Nakano, Koji Abe, Masaya Oda, Masaaki Konagaya, Takashi Imai, Masanori Nakagawa, Takuji Fujita, Hidenao Sasaki, and Masatoyo Nishizawa.

Acknowledgments

We thank all the family members for participating in this study. This study was supported in part by KAKENHI (Grants-in-Aid for Scientific Research on Innovative Areas [22129001 and 22129002]) to S.T.; the Global COE Program from the Ministry of Education, Culture, Sports, Science, and Technology of Japan, and a grant-in-aid (H23-Jitsuyoka [Nanbyo]-Ippan-004) from the Ministry of Health, Labour, and Welfare, Japan to S.T. We acknowledge support to R.H.B. from ALS Therapy Alliance, Project ALS, P2ALS, the Angel Fund, the Pierre L. de Bourgknecht ALS Research Foundation, the Al-Athel ALS Research Foundation, the ALS Family Charitable Foundation, and grant 1R01NS050557 from the National Institute of Neurological Disorders and Stroke of the National Institutes of Health and support to G.A.N. from the MND Research Institute of Australia. P.G.-P. was supported by the Alfonso Martin Escudero Foundation (Madrid).

Received: May 12, 2013
Revised: August 26, 2013
Accepted: September 13, 2013
Published: October 10, 2013

Web Resources

The URLs for data presented herein are as follows:

1000 Genomes Project Database, http://www.1000genomes.org/
dbSNP135, http://www.ncbi.nlm.nih.gov/projects/SNP/
ExonPrimer, http://ihg.gsf.de/ihg/ExonPrimer.html
NCBI37/hg19 assembly, http://genome.ucsc.edu/
NHLBI GO Exome Sequencing Project (NHLBI-ESP), https://esp.gs.washington.edu/drupal
Online Mendelian Inheritance in Man (OMIM), http://www.omim.org/
Personal genome databases, http://www.sequenceontology.org/resources/10Gen.html
PLINK algorithm, http://pngu.mgh.harvard.edu/purcell/plink/
PolyPhen-2, http://genetics.bwh.harvard.edu/pph2/
Refseq, http://www.ncbi.nlm.nih.gov/projects/RefSeq/
UCSC Human Genome Browser, http://genome.ucsc.edu/

Accession Numbers

The dbSNP accession numbers for the c. 2780G>A and c. 3823C>T mutations reported for *ERBB4* in this paper are ss831884245 and ss831884246, respectively.

References

1. Al-Chalabi, A., Jones, A., Troakes, C., King, A., Al-Sarraj, S., and van den Berg, L.H. (2012). The genetics and neuropathology of amyotrophic lateral sclerosis. Acta Neuropathol. *124*, 339–352.
2. Andersen, P.M., and Al-Chalabi, A. (2011). Clinical genetics of amyotrophic lateral sclerosis: what do we really know? Nat Rev Neurol *7*, 603–615.
3. Takahashi, Y., Seki, N., Ishiura, H., Mitsui, J., Matsukawa, T., Kishino, A., Onodera, O., Aoki, M., Shimozawa, N., Murayama, S., et al. (2008). Development of a high-throughput microarray-based resequencing system for neurological disorders and its application to molecular genetics of amyotrophic lateral sclerosis. Arch. Neurol. *65*, 1326–1332.
4. Ishiura, H., Takahashi, Y., Mitsui, J., Yoshida, S., Kihira, T., Kokubo, Y., Kuzuhara, S., Ranum, L.P., Tamaoki, T., Ichikawa, Y., et al. (2012). C9ORF72 repeat expansion in amyotrophic lateral sclerosis in the Kii peninsula of Japan. Arch. Neurol. *69*, 1154–1158.
5. Li, H., and Durbin, R. (2009). Fast and accurate short read alignment with Burrows-Wheeler transform. Bioinformatics *25*, 1754–1760.
6. Li, H., Handsaker, B., Wysoker, A., Fennell, T., Ruan, J., Homer, N., Marth, G., Abecasis, G., and Durbin, R.; 1000 Genome Project Data Processing Subgroup. (2009). The Sequence Alignment/Map format and SAMtools. Bioinformatics *25*, 2078–2079.
7. Robinson, J.T., Thorvaldsdóttir, H., Winckler, W., Guttman, M., Lander, E.S., Getz, G., and Mesirov, J.P. (2011). Integrative genomics viewer. Nat. Biotechnol. *29*, 24–26.
8. Fukuda, Y., Nakahara, Y., Date, H., Takahashi, Y., Goto, J., Miyashita, A., Kuwano, R., Adachi, H., Nakamura, E., and Tsuji, S. (2009). SNP HiTLink: a high-throughput linkage analysis system employing dense SNP data. BMC Bioinformatics *10*, 121.
9. Gudbjartsson, D.F., Thorvaldsson, T., Kong, A., Gunnarsson, G., and Ingolfsdottir, A. (2005). Allegro version 2. Nat. Genet. *37*, 1015–1016.
10. Purcell, S., Neale, B., Todd-Brown, K., Thomas, L., Ferreira, M.A., Bender, D., Maller, J., Sklar, P., de Bakker, P.I., Daly, M.J., and Sham, P.C. (2007). PLINK: a tool set for whole-genome association and population-based linkage analyses. Am. J. Hum. Genet. *81*, 559–575.

11. Kong, A., Frigge, M.L., Masson, G., Besenbacher, S., Sulem, P., Magnusson, G., Gudjonsson, S.A., Sigurdsson, A., Jonasdottir, A., Jonasdottir, A., et al. (2012). Rate of de novo mutations and the importance of father's age to disease risk. Nature *488*, 471–475.
12. Sanders, S.J., Murtha, M.T., Gupta, A.R., Murdoch, J.D., Raubeson, M.J., Willsey, A.J., Ercan-Sencicek, A.G., DiLullo, N.M., Parikshak, N.N., Stein, J.L., et al. (2012). De novo mutations revealed by whole-exome sequencing are strongly associated with autism. Nature *485*, 237–241.
13. Plowman, G.D., Green, J.M., Culouscou, J.M., Carlton, G.W., Rothwell, V.M., and Buckley, S. (1993). Heregulin induces tyrosine phosphorylation of HER4/p180erbB4. Nature *366*, 473–475.
14. Carpenter, G. (2003). ErbB-4: mechanism of action and biology. Exp. Cell Res. *284*, 66–77.
15. Sundvall, M., Korhonen, A., Vaparanta, K., Anckar, J., Halkilahti, K., Salah, Z., Aqeilan, R.I., Palvimo, J.J., Sistonen, L., and Elenius, K. (2012). Protein inhibitor of activated STAT3 (PIAS3) protein promotes SUMOylation and nuclear sequestration of the intracellular domain of ErbB4 protein. J. Biol. Chem. *287*, 23216–23226.
16. Pearson, R.J., Jr., and Carroll, S.L. (2004). ErbB transmembrane tyrosine kinase receptors are expressed by sensory and motor neurons projecting into sciatic nerve. J. Histochem. Cytochem. *52*, 1299–1311.
17. Gassmann, M., Casagranda, F., Orioli, D., Simon, H., Lai, C., Klein, R., and Lemke, G. (1995). Aberrant neural and cardiac development in mice lacking the ErbB4 neuregulin receptor. Nature *378*, 390–394.
18. Golub, M.S., Germann, S.L., and Lloyd, K.C.K. (2004). Behavioral characteristics of a nervous system-specific erbB4 knockout mouse. Behav. Brain Res. *153*, 159–170.
19. Wolpowitz, D., Mason, T.B., Dietrich, P., Mendelsohn, M., Talmage, D.A., and Role, L.W. (2000). Cysteine-rich domain isoforms of the neuregulin-1 gene are required for maintenance of peripheral synapses. Neuron *25*, 79–91.
20. Yang, X., Arber, S., William, C., Li, L., Tanabe, Y., Jessell, T.M., Birchmeier, C., and Burden, S.J. (2001). Patterning of muscle acetylcholine receptor gene expression in the absence of motor innervation. Neuron *30*, 399–410.
21. Song, F., Chiang, P., Wang, J., Ravits, J., and Loeb, J.A. (2012). Aberrant neuregulin 1 signaling in amyotrophic lateral sclerosis. J. Neuropathol. Exp. Neurol. *71*, 104–115.

J Neurol (2013) 260:2917–2927
DOI 10.1007/s00415-013-7112-y

Amyotrophic lateral sclerosis: an update on recent genetic insights

Yohei Iguchi · Masahisa Katsuno · Kensuke Ikenaka · Shinsuke Ishigaki · Gen Sobue

Received: 31 August 2013 / Revised: 10 September 2013 / Accepted: 12 September 2013 / Published online: 2 October 2013

Abstract Amyotrophic lateral sclerosis (ALS) is a devastating neurodegenerative disease affecting both upper and lower motor neurons. The prognosis for ALS is extremely poor, but there is a limited course of treatment with only one approved medication. A most striking recent discovery is that TDP-43 is identified as a key molecule that is associated with both sporadic and familial forms of ALS. TDP-43 is not only a pathological hallmark, but also a genetic cause for ALS. Subsequently, a number of ALS-causative genes have been found. Above all, the RNA-binding protein, such as FUS, TAF15, EWSR1 and hnRNPA1, have structural and functional similarities to TDP-43, and physiological functions of some molecules, including *VCP, UBQLN2, OPTN, FIG4* and *SQSTM1,* are involved in a protein degradation system. These discoveries provide valuable insight into the pathogenesis of ALS, and open doors for developing an effective disease-modifying therapy.

Keywords Amyotrophic lateral sclerosis · Motor neuron disease · Protein aggregation · RNA metabolism

Y. Iguchi · M. Katsuno · K. Ikenaka · S. Ishigaki · G. Sobue (✉)
Department of Neurology, Nagoya University Graduate School of Medicine, 65 Tsurumai-cho, Showa-ku, Nagoya 466-8550, Japan
e-mail: sobueg@med.nagoya-u.ac.jp

Y. Iguchi
The Centre de Recherche de l'Institut Universitaire en Santé Mentale de Québec-CRIUSMQ, Laval University, Quebec, QC G1J 2G3, Canada

Introduction

Amyotrophic lateral sclerosis (ALS) is an adult-onset, progressive, and devastating neurodegenerative disease. The typical ALS case develops a muscle weakness and atrophy, which result from selective motor neuronal death in the cortex, brain stem, and spinal cord, but does not affect the oculomotor, sensory or autonomic functions. ALS occurs alone or with frontotemporal lobar degeneration (FTLD). Transactive response (TAR)-DNA binding protein 43 kDa (TDP-43) was identified as a component of the ubiquitinated neuronal inclusion in sporadic ALS (SALS) and FTLD with ubiquitinated inclusions [1–3]. These two diseases have been regarded as part of the spectrum of a single disease referred to as TDP-43 proteinopathy. TDP-43 is reported to be a causative molecule of familial ALS (FALS) [4–7]. Subsequently, a number of ALS-causative genes have been identified (http://neuromuscular.wustl.edu/index.html). Some of the identified ALS-causative molecules share physiological roles indispensable for a cellular activity and are involved in SALS pathologies (Fig. 1). Although the cause of SALS, which accounts for ~90 % of ALS, is uncertain, these discoveries have provided novel insights into the pathogenesis of ALS. Here we review recent genetic findings concering ALS.

TARDBP

In 2006, two groups reported that TDP-43 is a major component of ubiquitinated neuronal cytoplasmic inclusions in both SALS and FTLD [1, 2]. In addition, mutations of *TARDBP,* the gene encoding TDP-43, cause an autosomal dominant FALS, which accounts for ~5 % of FALS

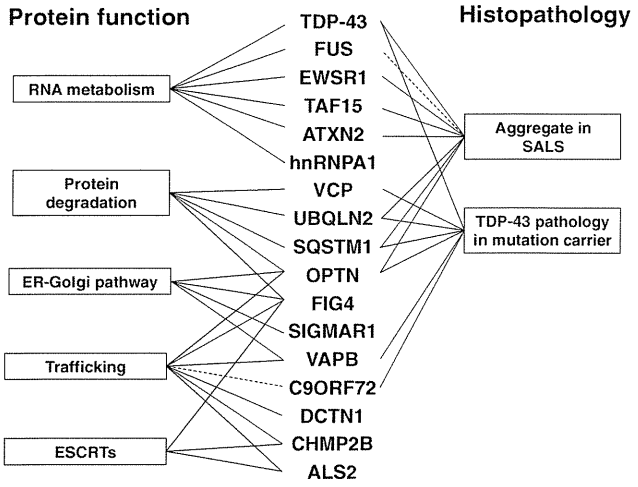

Fig. 1 Physiological and neuropathological overlaps of ALS-causative genes. Several ALS-causing molecules share similar cellular functions and are possibly co-localized in intra-neuronal aggregates of ALS. Aggregate in SALS; the protein encoded by each gene forms aggregates in a SALS-affected region. TDP-43 pathology in mutation carrier; TDP-43-positive cytoplasmic inclusion is observed in ALS cases with each mutation. ESCRTs, endosomal sorting complexes required for transport

cases [4–7]. Except for D169G, all *TARDBP* mutations are in the C-terminal glycine-rich region encoded by exon 6. Although ALS patients carrying TDP-43 mutations normally exhibit a classical ALS phenotype with rare co-occurrence of dementia, there is a trend for disease onset to be earlier, with upper limb onset being more common and a longer duration compared to SALS patients [8]. TDP-43 is an RNA-binding protein that regulates elements of RNA metabolism such as gene transcription, stability of mRNA, pre-mRNA splicing, and microRNA biogenesis [9–18]. This protein is redistributed from the nucleus to the cytoplasm and forms aggregates in affected neurons and glial cells of SALS patients [1–3] (Fig. 2), suggesting that gain and/or loss of TDP-43 function underlies SALS pathogenesis. With regard to gain of TDP-43 toxicity, rodent and primate models overexpressing wild-type or disease-mutant TDP-43 exhibit the phenotype of neurodegeneration, but this exogenous TDP-43 exists mainly in the nuclei, and TDP-43-positive cytoplasmic inclusions are barely detectable [19–28]. Although it is unclear how wild-type and mutant TDP-43 acquire a toxic effect, overexpression of TDP-43 makes a dose-dependent contribution to neurodegeneration [20–22]. In addition, pathological *TARDBP* mutations have longer half-lives compared to the wild type [29, 30], and longer half-lives of mutant proteins are correlated with accelerated disease onset [30], suggesting that mutant TDP-43 toxicity depends on its protein stability. On the other hand, *TARDBP* knockout mice are embryonic lethal [31–33], and postnatal deletion of *TARDBP* led to rapid loss of body fat and death [34]. Finally, motor neuron-specific *TARDBP* knockout mice exhibited age-dependent progressive motor dysfunction together with ALS-mimicking pathology, including motor axonal degeneration, neurogenic muscle atrophy, and denervation at neuromuscular junctions [35, 36] (Fig. 3). These lines of evidence suggest that both gain and loss of TDP-43 function contribute to ALS pathogenesis.

FUS

Mutations in the gene encoding fused in sarcoma (FUS) mutations have been identified in autosomal dominant FALS, which accounts for ~4 % of FALS cases [37–39]. The majority of *FUS* mutations are in the C-terminal nuclear localization signal (NLS), and these mutants cause aberrant cytoplasmic distributions of FUS [37, 38]. Although the majority of patients carrying *FUS* mutations exhibit a classical ALS phenotype without cognitive impairment, the clinical courses of these ALS patients are diverse, even among carriers of the same mutations [40–44]. The FUS protein has been demonstrated in neuronal cytoplasmic inclusions in ALS cases with *FUS* mutations and a subset of FTLD with ubiquitinated, neuronal intermediate filament inclusion disease (NINID), and basophilic

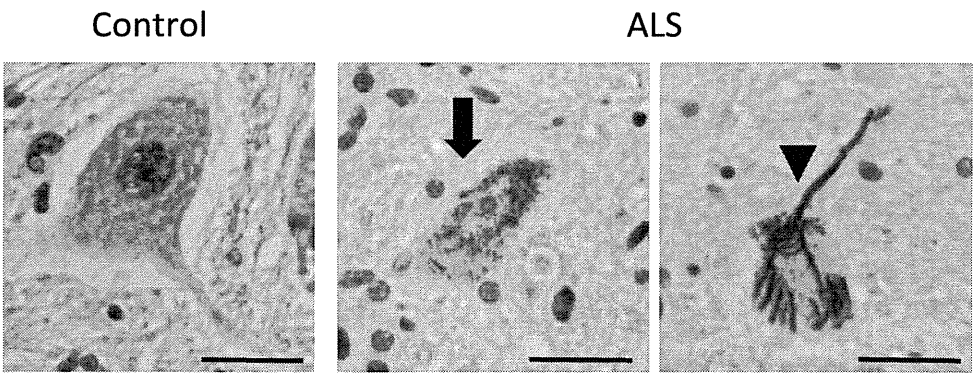

Fig. 2 TDP-43 pathology of spinal motor neuron. Lumbar spinal cords of control and ALS patients were stained with anti-TDP-43 antibody (Proteintech). TDP-43 is normally localized in the nucleus, but is redistributed to the cytoplasm in various patterns, such as a diffuse granular distribution (*arrow*) and skein-like inclusions (*arrow head*). The *scale bars* represent 20 μm

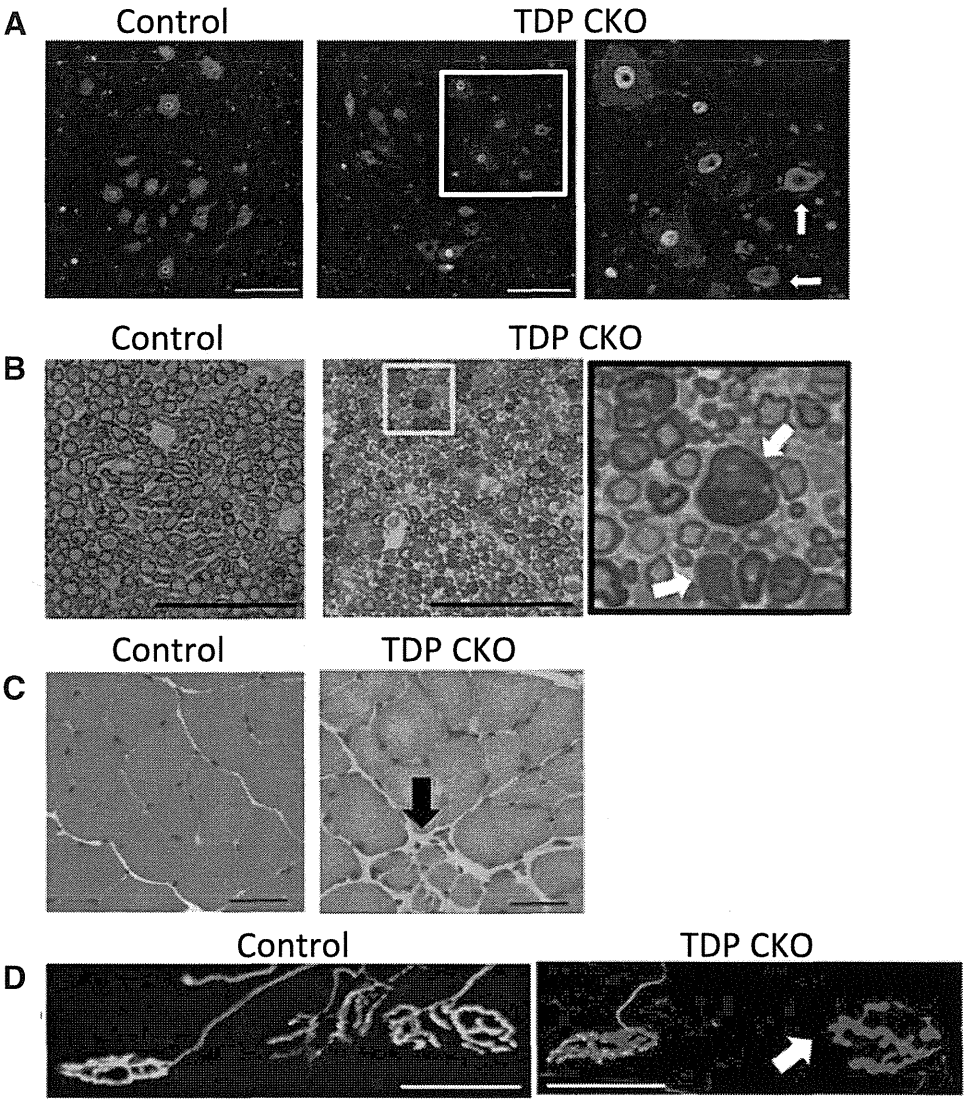

Fig. 3 Motor neuron-specific TDP-43 knockout (TDP CKO) mice exhibit degeneration of the motor neuron system. **a** Immunofluorescencent stainings (TDP-43, *green*; ChAT, *red*) of the lumbar ventral horn from 100-week-old control and TDP CKO mice. TDP-43-lacking motor neurons (*arrows*) were significantly smaller than TDP-43-positive motor neurons. **b** Toluidine blue-stained images in the L5 ventral root from 100-week-old control and TDP CKO mice. *Arrows* indicate axonal degeneration. The *scale bars* represent 100 μm. **c** Hematoxylin and eosin staining of gastrocnemius muscles of 100-week-old mice. Axial sections from TDP CKO mice exhibited grouped atrophy (*arrow*). **d** Immunofluorescent staining (synaptophysin and phopsho-neurofilament, *green*; bungarotoxin, *red*) of NMJs in 100-week-old mice. Denervated NMJs (*arrow*) are indicated by the lack of staining of synaptophysin and phospho-neurofilament. The *scale bar* represents 50 μm. Reproduced with permission from Iguchi et al. Ref. [36]

inclusion body disease (BIBD) [45–48]. These inclusions are positive for GRP78/BiP, p62 and ubiquitin, but not for TDP-43 [38, 49, 50]. In addition, FUS is reported to be co-localized with ubiquitin and TDP-43-positive cytoplasmic inclusions of SALS patients [51, 52]. This issue remains controversial, however, because in other studies, FUS was not found in these inclusions in SALS [38, 47, 53]. Rat models overexpressing human disease mutants of *FUS* exhibit pathological phenotypes like ALS and FTLD [54], and overexpression of human wild-type FUS in mice causes dose-dependent progressive motor neuron degeneration [55]. By contrast, *FUS* knockout mice on an inbred C57BL/6 background display perinatal death and exhibit abnormal lymphocytes and chromosomal instability [56], whereas knockout mice on an outbred background develop male sterility and survive until adulthood [57]. It is noteworthy that FUS and TDP-43 share structural and functional similarities [58] and that both proteins regulate alternative pre-mRNA splicing events and transcription [59–62]. Although most of the mRNA targets for FUS are distinct from those for TDP-43, a small set of common targets may contribute to ALS pathogenesis [60, 61]. In addition, both TDP-43 and FUS associate with the SMN complex and are involved in spliceosome maintenance [63, 64].

FIG4

FIG4 was reported as a causative gene for Charcot-Marie-Tooth disease type 4J (CMT4J), an autosomal recessive motor and sensory neuropathy [65]. Later, *FIG4* mutations were identified in autosomal-dominant FALS and SALS [66]. In this cohort of European ancestry, *FIG4* mutations were found in 2 % of ALS and primary lateral sclerosis (PLS) cases [66]. Two of ten identified mutations are truncation mutations that lead to loss of FIG4 phosphatase

activity [66]. The protein transcript of *FIG4* is a phosphoinositide 5-phosphatase that regulates a cellular abundance of phosphatidylinositol 3,5-bisphosphate (PI(3,5)P2), a signaling lipid on the cytosolic surface of membranes of the late endosomal compartment [67]. PI(3,5)P2 is required for retrograde membrane trafficking from lysosomal and late endosomal compartments to the Golgi and is involved in autophagy [68–70]. The analysis of $FIG4^{-/-}$ mouse brain shows disruption of autophagy in neurons and glial cells [71].

OPTN

Three mutations of *OPTN* were identified in Japanese FALS patients [72], with both dominant and recessive mutations observed. Later analyses in Japanese and European populations revealed several additional mutations, and estimated mutation rates were 1–4 % in FALS [73–75]. Although optineurin, which is encoded by *OPTN,* regulates TNFα-induced NF-κB activation negatively by binding to polyubiquitinated RIP [76], ALS-causative *OPTN* mutations abolish its inhibition [72]. OPTN also acts as an autophagy receptor [77] and coordinates actin-based and microtubule-based motor function for maintenance of Golgi morphology [78]. OPTN is co-localized in ubiquitinated neuronal cytoplasmic inclusions of SALS spinal cords [72, 79–81], suggesting that OPTN is generally involved in the pathogenesis of a variety of ALS types.

ATXN2

The pathological expansions (>34 repeats) of a CAG repeat in *ATXN2,* which encodes a polyglutamine tract in ataxin-2, cause spinocerebellar ataxia type 2 (SCA2). Intermediate-length expansions (27–33 glutamine residues) were reported to contribute to susceptibility to ALS [82]. In a later study, however, longer *ATXN2* repeats (>29–32 repeats) were significantly associated with the disease [83–86], and CAG repeats (≥32) were found in approximately 2 % of familial and sporadic ALS patients [84]. Furthermore, Expanded *ATXN2* repeats were also significantly associated with progressive supranuclear palsy [87]. Pathological analysis shows that ataxin-2 forms cytoplasmic aggregates in ALS spinal cord neurons, although this protein is localized in a diffuse or fine-granular pattern throughout the cytoplasm of control spinal cord neurons [82]. Although the pathological mechanism of *ATXN2* expansion in ALS pathogenesis is not fully understood, CAG repeat expansions are reported to enhance the interaction between ataxin-2 and TDP-43 or mutant FUS [82, 88].

DAO

D-serine, a co-agonist of the *N*-methyl D-aspartate (NMDA) type of glutamate receptor [89], was reported to accumulate in the spinal cords of SALS and G93A SOD1 mice [90, 91]. D-amino acid oxidase (DAO) negatively regulates D-serine. Mutation R199W in the *DAO* gene was identified in autosomal dominant FALS [92]. This mutation, when expressed in neuronal cell lines, reduces cell viabilities and induces ubiquitinated aggregates [92]. These data suggest that accumulation of D-serine contributes to an ALS pathogenesis, and DAO might be a common therapeutic target for ALS.

SPG11

Mutations of the spatacsin gene (*SPG11*) are the most common cause of hereditary spastic paraplegia with thinning corpus callosum [93]. Recently, *SPG11* mutations were identified in autosomal recessive juvenile ALS [94]. These patients exhibit a slowly progressive phenotype of motor neuron disease. Although the loss-of-function mechanism is suggested as the pathogenesis of ALS with the *SPG11* mutation, the physiological function of this molecule is unclear.

VCP

Mutations in *VCP* were found in patients with inclusion body myopathy of early-onset Paget disease and frontotemporal dementia (IBMPFD) [95]. In addition, *VCP* mutation was identified in 1–2 % of FALS cases with or without the phenotype of IBMPFD in an autosomal dominant manner [96]. Now, IBMPFD is referred to as a multisystem proteinopathy (MSP), which affects motor neurons, brain, skeletal muscle, and bone. *VCP* mutation carriers exhibit diverse phenotypes, even with the same mutation [97]. TDP-43 positive ubiquitinated cytoplasmic inclusions in the affected neurons are present in patients with *VCP* mutations [96, 98]. The highly conserved AAA+-ATPase, VCP regulates multiple cellular pathways such as the ubiquitin–proteasome system (UPS), autophagy, endosomal sorting, and regulating protein degradation at the outer mitochondrial membrane, and chromatin-associated processes [99]. VCP is indispensable for maturation of autophagosomes, and disease-causative mutations of VCP disrupt this process [100]. Mutant VCP knock-in mice develop age-dependent motor dysfunction with abnormal TDP-43 pathologies in the spinal cord, muscle and brain [101–103].

UBQLN2

Mutations in *UBQLN2* were identified in rare X-linked dominant ALS cases [104]. UBQLN2-positive inclusions are found in the spinal cord of ALS and ALS/FTLD patients with *UBQLN2* mutations, and these inclusions frequently contain TDP-43 and FUS [104, 105]. In addition, abnormal UBQLN2 pathologies are found in SALS patients and FUS mutation carriers [104, 105]. These data suggest that UBQLN2 is generally involved in the pathogenesis of ALS. UBQLN2 is a member of the ubiquilin family, which is involved in both the ubiquitin–proteasome system and autophagy [106, 107], and mutations in *UBQLN2* were reported to disrupt protein degradation [104].

C9ORF72

In a large family with FTLD and/or ALS mapping to chromosome 9p21, a GGGGCC hexanucleotide repeat was identified between noncoding exons 1a and 1b of the *C9ORF72* gene [108, 109]. The repeat is <25 units in healthy controls, whereas the estimated expansion range is from 800 to 4,400 units in cases carrying this repeat expansion [108–110]. The mutation frequencies in European and North American Caucasian populations are generally high: they are up to 29, 50 and 88 % in FTLD, ALS and ALS/FTLD patients [111]. Especially in North Europe, the repeat expansion frequencies are from 12 to 21 %, even in the SALS patients [108, 112, 113]. By contrast, the frequency of ALS patients with these expansions is very low in Asian populations [113–119]. ALS patients with C9ORF72 expansion commonly have a bulbar onset and cognitive impairment and partially exhibit Parkinsonism or psychiatric symptoms such as psychosis or suicide [120–122]. Abundant UBQLN-positive cytoplasmic inclusions are seen in the cerebellum and the hippocampus. UBQLN is co-localized partially with p62 and only rarely with TDP-43 positive inclusions [123, 124]. Using RNA fluorescence in situ hybridization (FISH) analysis, C9ORF72-containing RNA foci are observed in 25 % of the spinal cord and frontal cortical neurons of patients with the repeat expansion [108]. In addition, the neurons contain dipeptide repeat proteins generated from this intronic repeat region by non-ATG-initiated translation [125, 126]. It is, however, uncertain whether these neuronal accumulations of the aberrant RNA, and protein derived from C9ORF72 repeat expansions contribute to the neurodegeneration. The latest study demonstrated that C9ORF72 is a full-length distant homologue of proteins related to DENN, which is a Rab GEF, a regulator of Rab-GTPase activity [127]. Because Rab GTPases regulate membrane trafficking, C9ORF72 may have a crucial role in neuronal activities such as axonal transport and the autophagy-lysosome system. Although no reliable antibody for this protein is known, the intronic repeat expansions are reported to cause the loss of one or all alternatively spliced C9ORF72 transcripts [108, 109, 128], suggesting that C9ORF72 haploinsufficiency may underlie the pathogenesis of ALS patients carrying this repeat expansion. The high incidence of C9ORF72 mutations in Caucasian ALS patients raises the possibility of the additional identification for ALS-causative gene mutations, even in SALS. Targeting a specific molecule, such as C9ORF72, appears to be a promising strategy.

PFN1

PFN1 mutations were identified in autosomal dominant FALS patients, [129]. Although four missense mutations were reported in 274 FALS patients [129], several other analyses further suggest that the mutation carriers in FALS patients are generally rare [130–138]. Profilin-1, the protein transcript of *PFN1*, is essential for the polymerization of monomeric G-actin to form filamentous actin [139]. A disrupted mutant of *PFN1* causes a growth cone arrest in embryonic motor neurons of Drosophila [140]. Although the neuropathology of an ALS patient with the *PFN1* mutation is not reported, ALS-related mutants of *PFN1* form ubiquitinated cytoplasmic aggregates when they are overexpressed in Neuro-2a cells or primary motor neurons [129]. In addition, the *PFN1* mutants reduce actin-binding ability, inhibit axonal outgrowth, and reduce the size of the growth cone in cultured cells or primary motor neurons [129]. These findings suggest that mutation-dependent disruption of *PFN1* function contributes to ALS pathogenesis via an alteration of the actin dynamic pathway.

SIGMAR1

SIGMAR1 is reported to be associated with juvenile amyotrophic sclerosis. A homozygous missense mutation, E102Q, in *SIGMAR1* gene was identified in autosomal recessive FALS from Saudi Arabia [141]. Patients carrying the *SIGMAR1* mutation exhibit the motor neuron disease phenotype at the age of 1–2 years, and the weakness progresses slowly without cognitive impairment. The sigma-1 receptor (S1R), which is encoded by *SIGMAR1*, is a non-steroidal ER protein that regulates various ion channel activities and has a protein chaperone function [142]. S1R is highly expressed in motor neurons of the brain stem and spinal cord, and S1R knockout mice are reported to have motor deficiency [143]. These findings suggest that the mutation in *SIGMAR1* affects predominantly motor neurons via loss of S1R function. Further investigations,

including a histopathological characterization of post-mortem samples and functional analysis of the S1R mutant, are needed.

Molecular targeted approach for the treatment of ALS

Current therapies for neurodegenerative diseases are targeted mainly to symptomatic relief or replacement of neurotransmitters. Most of these therapies, however, do not halt or reduce neurodegenerative progression [144]. With regard to ALS, the only available drug, riluzole (6-(trifluoromethoxy)benzothiazol-2-amine), has a limited effect: the increase in median survival for the riluzole-treated group was 2–3 months [145]. Many compounds, including vitamin E, gabapentin, topiramate, creatine, celecoxib and minocycline, identified in studies using animal models have failed in the clinical trials of ALS.

Although several interpretations can be considered, one possibility of the cause of this divergence is the use of mutant SOD1 mice in pre-clinical studies. There are distinct pathophysiological differences between SOD1-mediated FALS (ALS1) and SALS [146, 147]. Conversely, TDP-43 is a promising therapeutic target for SALS, because abnormal TDP-43 pathologies are characteristic features of SALS. Given that a dose-dependent or aggregate toxicity of TDP-43 would be related to ALS pathogenesis, interventions to regulate TDP-43 protein expression or to mitigate the aggregate formation could have therapeutic potential for ALS. An analysis using induced pluripotent stem (iPS) cells derived from ALS patients carrying TDP-43 mutations would be a useful tool for elucidating ALS disease pathogenesis and for screening drug candidates [148].

Analyzing functional similarities to ALS-causative molecules is a promising approach. Some of these molecules share physiological functions indispensable for cellular activities, including RNA metabolism, protein degradation, and the ER-Golgi pathway (Fig. 1). For instance, several ALS-causative genes, including *VCP, UBQLN2, OPTN* and *FIG4,* are related to a protein-degrading system via autophagy, and mutations in *SQSTM1*, which encodes p62, have been identified in ALS patients [149]. ALS patients carrying mutations in these genes have TDP-43-positive neuronal cytoplasmic inclusions, suggesting that the effect of these mutations could be an upstream cause for the aberrant TDP-43 pathology. In addition, p62-positive neuronal inclusions are seen in most of SALS and FALS patients, and accumulations of autophagosomes are observed in the motor neurons of SALS patients [150]. These lines of data suggest that dysregulation of autophagy commonly underlies ALS pathogenesis. Notably, autophagy activators rescue the phenotype and pathology in FTLD model mice in which wild-type TDP-43 was overexpressed in the forebrain [151], suggesting that the autophagic pathway could be a potential therapeutic target for ALS.

TDP-43, FUS, and ataxin-2 are components of stress granules (SGs), which have a central role in the stress response, such as regulating mRNA translation and turnover [152] under stress [153–155]. In addition, the TDP-43 C-terminal fragment and FUS-disease mutant are recruited more abundantly into SGs [156–158]. Given that stress granule marker proteins are co-localized in TDP-43 and FUS-positive neuronal inclusions of ALS and FTLD patients [158, 159], dysregulation of mRNA metabolism in SGs would underlie common ALS pathogenesis and could be a therapeutic target for ALS. Furthermore, TDP-43 and FUS have a similar sequence to the prion protein, prion-like domain (PrLD). Notably, an insoluble fraction of TDP-43 from FTLD brain has a seeding ability when introduced into cultured cells, and the aggregated TDP-43 induced by these seeds is propagated to neighboring cells [160]. These data suggest that interference with the propagation of TDP-43 or other RNA-binding proteins may be a therapeutic target for ALS. Finally, mutations in other RNA-binding proteins, such as Ewing's sarcoma breakpoint region 1 (EWSR1), TATA-binding protein-associated factor 15 (TAF15), and heterogeneous nuclear ribonucleoprotein A1 (hnRNPA1) have been identified in ALS patients [161–163]. These RNA-binding proteins are responsible for RNA metabolism and harbor a PrLD as well as TDP-43 and FUS.

ALS causative genes have been uncovered by recent developments in gene analysis technology. Certain FALS-causing gene mutations have also been identified in SALS cases, suggesting that sporadic and familial forms of ALS share, at least in part, the same molecular pathomechanism. These discoveries provide novel insight into ALS pathogenesis and are expected to contribute to developing an effective disease-modifying therapy. Given the limited availability of animal models carrying FALS mutations, the results of genetic studies should be utilized for the creation of models and the search for therapies that suppress motor neuron degeneration.

Acknowledgments This work was supported by Grant-in-Aids (KAKENHI) from the Ministry of Education, Culture, Sports, Science, and Technology of Japan (Nos. 22110005, 21229011 and 23390230) and Core Research for Evolutional Science and Technology (CREST) from the Japan Science and Technology Agency (JST). Figure 3 was reproduced from Iguchi et al. Ref. [36].

Conflicts of interest None.

References

1. Arai T, Hasegawa M, Akiyama H et al (2006) TDP-43 is a component of ubiquitin-positive tau-negative inclusions in

frontotemporal lobar degeneration and amyotrophic lateral sclerosis. Biochem Biophys Res Commun 351:602–611
2. Neumann M, Sampathu DM, Kwong LK et al (2006) Ubiquitinated TDP-43 in frontotemporal lobar degeneration and amyotrophic lateral sclerosis. Science 314:130–133
3. Mackenzie IR, Neumann M, Cairns NJ et al (2011) Novel types of frontotemporal lobar degeneration: beyond tau and TDP-43. J Mol Neurosci 45:402–408
4. Gitcho MA, Baloh RH, Chakraverty S et al (2008) TDP-43 A315T mutation in familial motor neuron disease. Ann Neurol 63:535–538
5. Kabashi E, Valdmanis PN, Dion P et al (2008) TARDBP mutations in individuals with sporadic and familial amyotrophic lateral sclerosis. Nat Genet 40:572–574
6. Sreedharan J, Blair IP, Tripathi VB et al (2008) TDP-43 mutations in familial and sporadic amyotrophic lateral sclerosis. Science 319:1668–1672
7. Yokoseki A, Shiga A, Tan CF et al (2008) TDP-43 mutation in familial amyotrophic lateral sclerosis. Ann Neurol 63:538–542
8. Corcia P, Valdmanis P, Millecamps S et al (2012) Phenotype and genotype analysis in amyotrophic lateral sclerosis with TARDBP gene mutations. Neurology 78:1519–1526
9. Wang HY, Wang IF, Bose J et al (2004) Structural diversity and functional implications of the eukaryotic TDP gene family. Genomics 83:130–139
10. Ayala YM, Pantano S, D'Ambrogio A et al (2005) Human, Drosophila, and C. elegans TDP43: nucleic acid binding properties and splicing regulatory function. J Mol Biol 348:575–588
11. Buratti E, Brindisi A, Giombi M et al (2005) TDP-43 binds heterogeneous nuclear ribonucleoprotein A/B through its C-terminal tail: an important region for the inhibition of cystic fibrosis transmembrane conductance regulator exon 9 splicing. J Biol Chem 280:37572–37584
12. Strong MJ, Volkening K, Hammond R et al (2007) TDP43 is a human low molecular weight neurofilament (hNFL) mRNA-binding protein. Mol Cell Neurosci 35:320–327
13. Buratti E, De Conti L, Stuani C et al (2010) Nuclear factor TDP-43 can affect selected microRNA levels. FEBS J 277:2268–2281
14. Polymenidou M, Lagier-Tourenne C, Hutt KR et al (2011) Long pre-mRNA depletion and RNA missplicing contribute to neuronal vulnerability from loss of TDP-43. Nat Neurosci 14:459–468
15. Tollervey JR, Curk T, Rogelj B et al (2011) Characterizing the RNA targets and position-dependent splicing regulation by TDP-43. Nat Neurosci 14:452–458
16. Sephton CF, Cenik C, Kucukural A et al (2011) Identification of neuronal RNA targets of TDP-43-containing ribonucleoprotein complexes. J Biol Chem 286:1204–1215
17. Xiao S, Sanelli T, Dib S et al (2011) RNA targets of TDP-43 identified by UV-CLIP are deregulated in ALS. Mol Cell Neurosci 47:167–180
18. Kawahara Y, Mieda-Sato A (2012) TDP-43 promotes microRNA biogenesis as a component of the Drosha and Dicer complexes. Proc Natl Acad Sci USA 109:3347–3352
19. Wegorzewska I, Bell S, Cairns NJ et al (2009) TDP-43 mutant transgenic mice develop features of ALS and frontotemporal lobar degeneration. Proc Natl Acad Sci USA 106:18809–18814
20. Wils H, Kleinberger G, Janssens J et al (2010) TDP-43 transgenic mice develop spastic paralysis and neuronal inclusions characteristic of ALS and frontotemporal lobar degeneration. Proc Natl Acad Sci USA 107:3858–3863
21. Xu YF, Gendron TF, Zhang YJ et al (2010) Wild-type human TDP-43 expression causes TDP-43 phosphorylation, mitochondrial aggregation, motor deficits, and early mortality in transgenic mice. J Neurosci 30:10851–10859
22. Stallings NR, Puttaparthi K, Luther CM et al (2010) Progressive motor weakness in transgenic mice expressing human TDP-43. Neurobiol Dis 40:404–414
23. Zhou H, Huang C, Chen H et al (2010) Transgenic rat model of neurodegeneration caused by mutation in the TDP gene. PLoS Genet 6:e1000887
24. Tsai KJ, Yang CH, Fang YH et al (2010) Elevated expression of TDP-43 in the forebrain of mice is sufficient to cause neurological and pathological phenotypes mimicking FTLD-U. J Exp Med 207:1661–1673
25. Shan X, Chiang PM, Price DL et al (2010) Altered distributions of Gemini of coiled bodies and mitochondria in motor neurons of TDP-43 transgenic mice. Proc Natl Acad Sci USA 107:16325–16330
26. Swarup V, Phaneuf D, Bareil C et al (2011) Pathological hallmarks of amyotrophic lateral sclerosis/frontotemporal lobar degeneration in transgenic mice produced with TDP-43 genomic fragments. Brain 134:2610–2626
27. Arnold ES, Ling SC, Huelga SC et al (2013) ALS-linked TDP-43 mutations produce aberrant RNA splicing and adult-onset motor neuron disease without aggregation or loss of nuclear TDP-43. Proc Natl Acad Sci USA 110:E736–E745
28. Uchida A, Sasaguri H, Kimura N et al (2012) Non-human primate model of amyotrophic lateral sclerosis with cytoplasmic mislocalization of TDP-43. Brain 135:833–846
29. Ling SC, Albuquerque CP, Han JS et al (2010) ALS-associated mutations in TDP-43 increase its stability and promote TDP-43 complexes with FUS/TLS. Proc Natl Acad Sci USA 107:13318–13323
30. Watanabe S, Kaneko K, Yamanaka K (2013) Accelerated disease onset with stabilized familial amyotrophic lateral sclerosis (ALS)-linked mutant TDP-43 proteins. J Biol Chem 288: 3641–3654
31. Wu LS, Cheng WC, Hou SC et al (2010) TDP-43, a neuropathosignature factor, is essential for early mouse embryogenesis. Genesis 48:56–62
32. Sephton CF, Good SK, Atkin S et al (2010) TDP-43 is a developmentally regulated protein essential for early embryonic development. J Biol Chem 285:6826–6834
33. Kraemer BC, Schuck T, Wheeler JM et al (2010) Loss of murine TDP-43 disrupts motor function and plays an essential role in embryogenesis. Acta Neuropathol 119:409–419
34. Chiang PM, Ling J, Jeong YH et al (2010) Deletion of TDP-43 down-regulates Tbc1d1, a gene linked to obesity, and alters body fat metabolism. Proc Natl Acad Sci USA 107:16320–16324
35. Wu LS, Cheng WC, Shen CK (2012) Targeted depletion of TDP-43 expression in the spinal cord motor neurons leads to the development of amyotrophic lateral sclerosis-like phenotypes in mice. J Biol Chem 287:27335–27344
36. Iguchi Y, Katsuno M, Niwa J et al (2013) Loss of TDP-43 causes age-dependent progressive motor neuron degeneration. Brain 136:1371–1382
37. Kwiatkowski TJ Jr, Bosco DA, Leclerc AL et al (2009) Mutations in the FUS/TLS gene on chromosome 16 cause familial amyotrophic lateral sclerosis. Science 323:1205–1208
38. Vance C, Rogelj B, Hortobagyi T et al (2009) Mutations in FUS, an RNA processing protein, cause familial amyotrophic lateral sclerosis type 6. Science 323:1208–1211
39. Van Langenhove T, van der Zee J, Sleegers K et al (2010) Genetic contribution of FUS to frontotemporal lobar degeneration. Neurology 74:366–371
40. Yan J, Deng HX, Siddique N et al (2010) Frameshift and novel mutations in FUS in familial amyotrophic lateral sclerosis and ALS/dementia. Neurology 75:807–814

41. Mackenzie IR, Ansorge O, Strong M et al (2011) Pathological heterogeneity in amyotrophic lateral sclerosis with FUS mutations: two distinct patterns correlating with disease severity and mutation. Acta Neuropathol 122:87–98
42. Groen EJ, van Es MA, van Vught PW et al (2010) FUS mutations in familial amyotrophic lateral sclerosis in the Netherlands. Arch Neurol 67:224–230
43. Hara M, Minami M, Kamei S et al (2012) Lower motor neuron disease caused by a novel FUS/TLS gene frameshift mutation. J Neurol 259:2237–2239
44. Yamashita S, Mori A, Sakaguchi H et al (2012) Sporadic juvenile amyotrophic lateral sclerosis caused by mutant FUS/TLS: possible association of mental retardation with this mutation. J Neurol 259:1039–1044
45. Munoz DG, Neumann M, Kusaka H et al (2009) FUS pathology in basophilic inclusion body disease. Acta Neuropathol 118:617–627
46. Neumann M, Rademakers R, Roeber S et al (2009) A new subtype of frontotemporal lobar degeneration with FUS pathology. Brain 132:2922–2931
47. Neumann M, Roeber S, Kretzschmar HA et al (2009) Abundant FUS-immunoreactive pathology in neuronal intermediate filament inclusion disease. Acta Neuropathol 118:605–616
48. Seelaar H, Klijnsma KY, de Koning I et al (2010) Frequency of ubiquitin and FUS-positive, TDP-43-negative frontotemporal lobar degeneration. J Neurol 257:747–753
49. Tateishi T, Hokonohara T, Yamasaki R et al (2010) Multiple system degeneration with basophilic inclusions in Japanese ALS patients with FUS mutation. Acta Neuropathol 119:355–364
50. Suzuki N, Aoki M, Warita H et al (2010) FALS with FUS mutation in Japan, with early onset, rapid progress and basophilic inclusion. J Hum Genet 55:252–254
51. Deng HX, Zhai H, Bigio EH et al (2010) FUS-immunoreactive inclusions are a common feature in sporadic and non-SOD1 familial amyotrophic lateral sclerosis. Ann Neurol 67:739–748
52. Keller BA, Volkening K, Droppelmann CA et al (2012) Co-aggregation of RNA binding proteins in ALS spinal motor neurons: evidence of a common pathogenic mechanism. Acta Neuropathol 124:733–747
53. Huang EJ, Zhang J, Geser F et al (2010) Extensive FUS-immunoreactive pathology in juvenile amyotrophic lateral sclerosis with basophilic inclusions. Brain Pathol 20:1069–1076
54. Huang C, Zhou H, Tong J et al (2011) FUS transgenic rats develop the phenotypes of amyotrophic lateral sclerosis and frontotemporal lobar degeneration. PLoS Genet 7:e1002011
55. Mitchell JC, McGoldrick P, Vance C et al (2013) Overexpression of human wild-type FUS causes progressive motor neuron degeneration in an age- and dose-dependent fashion. Acta Neuropathol 125:273–288
56. Hicks GG, Singh N, Nashabi A et al (2000) FUS deficiency in mice results in defective B-lymphocyte development and activation, high levels of chromosomal instability, and perinatal death. Nat Genet 24:175–179
57. Kuroda M, Sok J, Webb L et al (2000) Male sterility and enhanced radiation sensitivity in TLS (−/−) mice. EMBO J 19:453–462
58. Lagier–Tourenne C, Cleveland DW (2009) Rethinking ALS: the FUS about TDP-43. Cell 136:1001–1004
59. Ishigaki S, Masuda A, Fujioka Y et al (2012) Position-dependent FUS-RNA interactions regulate alternative splicing events and transcriptions. Sci Rep 2:529
60. Lagier–Tourenne C, Polymenidou M, Hutt KR et al (2012) Divergent roles of ALS-linked proteins FUS/TLS and TDP-43 intersect in processing long pre-mRNAs. Nat Neurosci 15:1488–1497
61. Rogelj B, Easton LE, Bogu GK et al (2012) Widespread binding of FUS along nascent RNA regulates alternative splicing in the brain. Sci Rep 2:603
62. Nakaya T, Alexiou P, Maragkakis M et al (2013) FUS regulates genes coding for RNA-binding proteins in neurons by binding to their highly conserved introns. RNA 19:498–509
63. Tsuiji H, Iguchi Y, Furuya A et al (2013) Spliceosome integrity is defective in the motor neuron diseases ALS and SMA. EMBO Mol Med 5:221–234
64. Yamazaki T, Chen S, Yu Y et al (2012) FUS-SMN protein interactions link the motor neuron diseases ALS and SMA. Cell Rep 2:799–806
65. Chow CY, Zhang Y, Dowling JJ et al (2007) Mutation of FIG4 causes neurodegeneration in the pale tremor mouse and patients with CMT4 J. Nature 448:68–72
66. Chow CY, Landers JE, Bergren SK et al (2009) Deleterious variants of FIG4, a phosphoinositide phosphatase, in patients with ALS. Am J Hum Genet 84:85–88
67. Volpicelli–Daley L, De Camilli P (2007) Phosphoinositides' link to neurodegeneration. Nat Med 13:784–786
68. Rutherford AC, Traer C, Wassmer T et al (2006) The mammalian phosphatidylinositol 3-phosphate 5-kinase (PIKfyve) regulates endosome-to-TGN retrograde transport. J Cell Sci 119:3944–3957
69. Zhang Y, Zolov SN, Chow CY et al (2007) Loss of Vac14, a regulator of the signaling lipid phosphatidylinositol 3,5-bisphosphate, results in neurodegeneration in mice. Proc Natl Acad Sci USA 104:17518–17523
70. Ferguson CJ, Lenk GM, Meisler MH (2010) PtdIns(3,5)P2 and autophagy in mouse models of neurodegeneration. Autophagy 6:170–171
71. Ferguson CJ, Lenk GM, Meisler MH (2009) Defective autophagy in neurons and astrocytes from mice deficient in PI(3,5)P2. Hum Mol Genet 18:4868–4878
72. Maruyama H, Morino H, Ito H et al (2010) Mutations of optineurin in amyotrophic lateral sclerosis. Nature 465:223–226
73. Del Bo R, Tiloca C, Pensato V et al (2011) Novel optineurin mutations in patients with familial and sporadic amyotrophic lateral sclerosis. J Neurol Neurosurg Psychiatry 82:1239–1243
74. Millecamps S, Boillee S, Chabrol E et al (2011) Screening of OPTN in French familial amyotrophic lateral sclerosis. Neurobiol Aging 32(557):e511–e553
75. Iida A, Hosono N, Sano M et al (2012) Optineurin mutations in Japanese amyotrophic lateral sclerosis. J Neurol Neurosurg Psychiatry 83:233–235
76. Zhu G, Wu CJ, Zhao Y et al (2007) Optineurin negatively regulates TNFα-induced NF-κB activation by competing with NEMO for ubiquitinated RIP. Curr Biol 17:1438–1443
77. Wild P, Farhan H, McEwan DG et al (2011) Phosphorylation of the autophagy receptor optineurin restricts Salmonella growth. Science 333:228–233
78. Sahlender DA, Roberts RC, Arden SD et al (2005) Optineurin links myosin VI to the Golgi complex and is involved in Golgi organization and exocytosis. J Cell Biol 169:285–295
79. Deng HX, Bigio EH, Zhai H et al (2011) Differential involvement of optineurin in amyotrophic lateral sclerosis with or without SOD1 mutations. Arch Neurol 68:1057–1061
80. Hortobagyi T, Troakes C, Nishimura AL et al (2011) Optineurin inclusions occur in a minority of TDP-43 positive ALS and FTLD-TDP cases and are rarely observed in other neurodegenerative disorders. Acta Neuropathol 121:519–527
81. Osawa T, Mizuno Y, Fujita Y et al (2011) Optineurin in neurodegenerative diseases. Neuropathology 31:569–574
82. Elden AC, Kim HJ, Hart MP et al (2010) Ataxin-2 intermediate-length polyglutamine expansions are associated with increased risk for ALS. Nature 466:1069–1075

83. Lee T, Li YR, Ingre C et al (2011) Ataxin-2 intermediate-length polyglutamine expansions in European ALS patients. Hum Mol Genet 20:1697–1700
84. Daoud H, Belzil V, Martins S et al (2011) Association of long ATXN2 CAG repeat sizes with increased risk of amyotrophic lateral sclerosis. Arch Neurol 68:739–742
85. Gispert S, Kurz A, Waibel S et al (2012) The modulation of Amyotrophic Lateral Sclerosis risk by ataxin-2 intermediate polyglutamine expansions is a specific effect. Neurobiol Dis 45:356–361
86. Van Damme P, Veldink JH, van Blitterswijk M et al (2011) Expanded ATXN2 CAG repeat size in ALS identifies genetic overlap between ALS and SCA2. Neurology 76:2066–2072
87. Ross OA, Rutherford NJ, Baker M et al (2011) Ataxin-2 repeat-length variation and neurodegeneration. Hum Mol Genet 20:3207–3212
88. Farg MA, Soo KY, Warraich ST et al (2013) Ataxin-2 interacts with FUS and intermediate-length polyglutamine expansions enhance FUS-related pathology in amyotrophic lateral sclerosis. Hum Mol Genet 22:717–728
89. Henneberger C, Papouin T, Oliet SH et al (2010) Long-term potentiation depends on release of D-serine from astrocytes. Nature 463:232–236
90. Sasabe J, Chiba T, Yamada M et al (2007) D-serine is a key determinant of glutamate toxicity in amyotrophic lateral sclerosis. EMBO J 26:4149–4159
91. Sasabe J, Miyoshi Y, Suzuki M et al (2012) D-amino acid oxidase controls motoneuron degeneration through D-serine. Proc Natl Acad Sci USA 109:627–632
92. Mitchell J, Paul P, Chen HJ et al (2010) Familial amyotrophic lateral sclerosis is associated with a mutation in D-amino acid oxidase. Proc Natl Acad Sci USA 107:7556–7561
93. Stevanin G, Santorelli FM, Azzedine H et al (2007) Mutations in SPG11, encoding spatacsin, are a major cause of spastic paraplegia with thin corpus callosum. Nat Genet 39:366–372
94. Orlacchio A, Babalini C, Borreca A et al (2010) SPATACSIN mutations cause autosomal recessive juvenile amyotrophic lateral sclerosis. Brain 133:591–598
95. Watts GD, Wymer J, Kovach MJ et al (2004) Inclusion body myopathy associated with Paget disease of bone and frontotemporal dementia is caused by mutant valosin-containing protein. Nat Genet 36:377–381
96. Johnson JO, Mandrioli J, Benatar M et al (2010) Exome sequencing reveals VCP mutations as a cause of familial ALS. Neuron 68:857–864
97. Rohrer JD, Warren JD, Reiman D et al (2011) A novel exon 2 I27V VCP variant is associated with dissimilar clinical syndromes. J Neurol 258:1494–1496
98. Neumann M, Mackenzie IR, Cairns NJ et al (2007) TDP-43 in the ubiquitin pathology of frontotemporal dementia with VCP gene mutations. J Neuropathol Exp Neurol 66:152–157
99. Meyer H, Bug M, Bremer S (2012) Emerging functions of the VCP/p97 AAA-ATPase in the ubiquitin system. Nat Cell Biol 14:117–123
100. Ju JS, Fuentealba RA, Miller SE et al (2009) Valosin-containing protein (VCP) is required for autophagy and is disrupted in VCP disease. J Cell Biol 187:875–888
101. Badadani M, Nalbandian A, Watts GD et al (2010) VCP associated inclusion body myopathy and paget disease of bone knock-in mouse model exhibits tissue pathology typical of human disease. PLoS One 5. doi: 10.1371/journal.pone.0013183
102. Custer SK, Neumann M, Lu H et al (2010) Transgenic mice expressing mutant forms VCP/p97 recapitulate the full spectrum of IBMPFD including degeneration in muscle, brain, and bone. Hum Mol Genet 19:1741–1755
103. Yin HZ, Nalbandian A, Hsu CI et al (2012) Slow development of ALS-like spinal cord pathology in mutant valosin-containing protein gene knock-in mice. Cell Death Dis 3:e374
104. Deng HX, Chen W, Hong ST et al (2011) Mutations in UBQLN2 cause dominant X-linked juvenile and adult-onset ALS and ALS/dementia. Nature 477:211–215
105. Williams KL, Warraich ST, Yang S et al (2012) UBQLN2/ubiquilin 2 mutation and pathology in familial amyotrophic lateral sclerosis. Neurobiol Aging 33:2527 e2523–2510
106. Rothenberg C, Srinivasan D, Mah L et al (2010) Ubiquilin functions in autophagy and is degraded by chaperone-mediated autophagy. Hum Mol Genet 19:3219–3232
107. Lee DY, Brown EJ (2012) Ubiquilins in the crosstalk among proteolytic pathways. Biol Chem 393:441–447
108. DeJesus-Hernandez M, Mackenzie IR, Boeve BF et al (2011) Expanded GGGGCC hexanucleotide repeat in noncoding region of C9ORF72 causes chromosome 9p-linked FTD and ALS. Neuron 72:245–256
109. Renton AE, Majounie E, Waite A et al (2011) A hexanucleotide repeat expansion in C9ORF72 is the cause of chromosome 9p21-linked ALS-FTD. Neuron 72:257–268
110. Beck J, Poulter M, Hensman D et al (2013) Large C9orf72 hexanucleotide repeat expansions are seen in multiple neurodegenerative syndromes and are more frequent than expected in the UK population. Am J Hum Genet 92:345–353
111. Cruts M, Gijselinck I, Van Langenhove T et al (2013) Current insights into the C9orf72 repeat expansion diseases of the FTLD/ALS spectrum. Trends Neurosci
112. Smith BN, Newhouse S, Shatunov A et al (2013) The C9ORF72 expansion mutation is a common cause of ALS ± FTD in Europe and has a single founder. Eur J Hum Genet 21:102–108
113. Majounie E, Renton AE, Mok K et al (2012) Frequency of the C9orf72 hexanucleotide repeat expansion in patients with amyotrophic lateral sclerosis and frontotemporal dementia: a cross-sectional study. Lancet Neurol 11:323–330
114. Tsai CP, Soong BW, Tu PH et al (2012) A hexanucleotide repeat expansion in C9ORF72 causes familial and sporadic ALS in Taiwan. Neurobiol Aging 33:2232.e2211–2232.e2218
115. Ishiura H, Takahashi Y, Mitsui J et al (2012) C9ORF72 repeat expansion in amyotrophic lateral sclerosis in the Kii peninsula of Japan. Arch Neurol 69:1154–1158
116. Ogaki K, Li Y, Atsuta N et al (2012) Analysis of C9orf72 repeat expansion in 563 Japanese patients with amyotrophic lateral sclerosis. Neurobiol Aging 33(2527):e2511–e2526
117. Konno T, Shiga A, Tsujino A et al (2013) Japanese amyotrophic lateral sclerosis patients with GGGGCC hexanucleotide repeat expansion in C9ORF72. J Neurol Neurosurg Psychiatry 84:398–401
118. Jang JH, Kwon MJ, Choi WJ et al (2013) Analysis of the C9orf72 hexanucleotide repeat expansion in Korean patients with familial and sporadic amyotrophic lateral sclerosis. Neurobiol Aging 34(1311):e1317–e1319
119. Zou ZY, Li XG, Liu MS et al (2013) Screening for C9orf72 repeat expansions in Chinese amyotrophic lateral sclerosis patients. Neurobiol Aging 34(1710):e1715–e1716
120. Byrne S, Elamin M, Bede P et al (2012) Cognitive and clinical characteristics of patients with amyotrophic lateral sclerosis carrying a C9orf72 repeat expansion: a population-based cohort study. Lancet Neurol 11:232–240
121. Floris G, Borghero G, Cannas A et al (2012) Frontotemporal dementia with psychosis, parkinsonism, visuo-spatial dysfunction, upper motor neuron involvement associated to expansion of C9ORF72: a peculiar phenotype? J Neurol 259:1749–1751
122. Calvo A, Moglia C, Canosa A et al (2012) Amyotrophic lateral sclerosis/frontotemporal dementia with predominant

manifestations of obsessive-compulsive disorder associated to GGGGCC expansion of the c9orf72 gene. J Neurol 259:2723–2725
123. Al-Sarraj S, King A, Troakes C et al (2011) p62-positive, TDP-43-negative, neuronal cytoplasmic and intranuclear inclusions in the cerebellum and hippocampus define the pathology of C9orf72-linked FTLD and MND/ALS. Acta Neuropathol 122:691–702
124. Brettschneider J, Van Deerlin VM, Robinson JL et al (2012) Pattern of ubiquilin pathology in ALS and FTLD indicates presence of C9ORF72 hexanucleotide expansion. Acta Neuropathol 123:825–839
125. Mori K, Weng SM, Arzberger T et al (2013) The C9orf72 GGGGCC repeat is translated into aggregating dipeptide-repeat proteins in FTLD/ALS. Science 339:1335–1338
126. Ash PE, Bieniek KF, Gendron TF et al (2013) Unconventional translation of C9ORF72 GGGGCC expansion generates insoluble polypeptides specific to c9FTD/ALS. Neuron 77:639–646
127. Levine TP, Daniels RD, Gatta AT et al (2013) The product of C9orf72, a gene strongly implicated in neurodegeneration, is structurally related to DENN Rab-GEFs. Bioinformatics 29:499–503
128. Gijselinck I, Van Langenhove T, van der Zee J et al (2012) A C9orf72 promoter repeat expansion in a Flanders-Belgian cohort with disorders of the frontotemporal lobar degeneration-amyotrophic lateral sclerosis spectrum: a gene identification study. Lancet Neurol 11:54–65
129. Wu CH, Fallini C, Ticozzi N et al (2012) Mutations in the profilin 1 gene cause familial amyotrophic lateral sclerosis. Nature 488:499–503
130. Zou ZY, Sun Q, Liu MS et al (2013) Mutations in the profilin 1 gene are not common in amyotrophic lateral sclerosis of Chinese origin. Neurobiol Aging 34(1713):e1715–e1716
131. van Blitterswijk M, Baker MC, Bieniek KF et al (2013) Profilin-1 mutations are rare in patients with amyotrophic lateral sclerosis and frontotemporal dementia. Amyotroph Lateral Scler Frontotemporal Degener
132. Tiloca C, Ticozzi N, Pensato V et al (2013) Screening of the PFN1 gene in sporadic amyotrophic lateral sclerosis and in frontotemporal dementia. Neurobiol Aging 34:1517 e1519–1510
133. Lattante S, Le Ber I, Camuzat A et al (2013) Mutations in the PFN1 gene are not a common cause in patients with amyotrophic lateral sclerosis and frontotemporal lobar degeneration in France. Neurobiol Aging 34(1709):e1701–e1702
134. Ingre C, Landers JE, Rizik N et al (2013) A novel phosphorylation site mutation in profilin 1 revealed in a large screen of US, Nordic, and German amyotrophic lateral sclerosis/frontotemporal dementia cohorts. Neurobiol Aging 34(1708):e1701–e1706
135. Dillen L, Van Langenhove T, Engelborghs S et al (2013) Explorative genetic study of UBQLN2 and PFN1 in an extended Flanders-Belgian cohort of frontotemporal lobar degeneration patients. Neurobiol Aging 34(1711):e1711–e1715
136. Daoud H, Dobrzeniecka S, Camu W et al (2013) Mutation analysis of PFN1 in familial amyotrophic lateral sclerosis patients. Neurobiol Aging 34(1311):e1311–e1312
137. Chen Y, Zheng ZZ, Huang R et al (2013) PFN1 mutations are rare in Han Chinese populations with amyotrophic lateral sclerosis. Neurobiol Aging 34(1922):e1921–e1925
138. Yang S, Fifita JA, Williams KL et al (2013) Mutation analysis and immunopathological studies of PFN1 in familial and sporadic amyotrophic lateral sclerosis. Neurobiol Aging 34:2235. e2237–2235.e2210
139. Mockrin SC, Korn ED (1980) Acanthamoeba profilin interacts with G-actin to increase the rate of exchange of actin-bound adenosine 5′-triphosphate. Biochemistry 19:5359–5362
140. Wills Z, Marr L, Zinn K et al (1999) Profilin and the Abl tyrosine kinase are required for motor axon outgrowth in the Drosophila embryo. Neuron 22:291–299
141. Al-Saif A, Al-Mohanna F, Bohlega S (2011) A mutation in sigma-1 receptor causes juvenile amyotrophic lateral sclerosis. Ann Neurol 70:913–919
142. Hayashi T, Su TP (2007) Sigma-1 receptor chaperones at the ER-mitochondrion interface regulate Ca(2+) signaling and cell survival. Cell 131:596–610
143. Mavlyutov TA, Epstein ML, Andersen KA et al (2010) The sigma-1 receptor is enriched in postsynaptic sites of C-terminals in mouse motoneurons. An anatomical and behavioral study. Neuroscience 167:247–255
144. Katsuno M, Tanaka F, Sobue G (2012) Perspectives on molecular targeted therapies and clinical trials for neurodegenerative diseases. J Neurol Neurosurg Psychiatry 83:329–335
145. Miller RG, Mitchell JD, Moore DH (2012) Riluzole for amyotrophic lateral sclerosis (ALS)/motor neuron disease (MND). Cochrane Database Syst Rev 3:CD001447
146. Mackenzie IR, Bigio EH, Ince PG et al (2007) Pathological TDP-43 distinguishes sporadic amyotrophic lateral sclerosis from amyotrophic lateral sclerosis with SOD1 mutations. Ann Neurol 61:427–434
147. Tan CF, Eguchi H, Tagawa A et al (2007) TDP-43 immunoreactivity in neuronal inclusions in familial amyotrophic lateral sclerosis with or without SOD1 gene mutation. Acta Neuropathol 113:535–542
148. Egawa N, Kitaoka S, Tsukita K et al (2012) Drug screening for ALS using patient-specific induced pluripotent stem cells. Sci Transl Med 4:145ra104
149. Fecto F, Yan J, Vemula SP et al (2011) SQSTM1 mutations in familial and sporadic amyotrophic lateral sclerosis. Arch Neurol 68:1440–1446
150. Sasaki S (2011) Autophagy in spinal cord motor neurons in sporadic amyotrophic lateral sclerosis. J Neuropathol Exp Neurol 70:349–359
151. Wang IF, Guo BS, Liu YC et al (2012) Autophagy activators rescue and alleviate pathogenesis of a mouse model with proteinopathies of the TAR DNA-binding protein 43. Proc Natl Acad Sci USA 109:15024–15029
152. Anderson P, Kedersha N (2008) Stress granules: the Tao of RNA triage. Trends Biochem Sci 33:141–150
153. Colombrita C, Zennaro E, Fallini C et al (2009) TDP-43 is recruited to stress granules in conditions of oxidative insult. J Neurochem 111:1051–1061
154. Andersson MK, Stahlberg A, Arvidsson Y et al (2008) The multifunctional FUS, EWS and TAF15 proto-oncoproteins show cell type-specific expression patterns and involvement in cell spreading and stress response. BMC Cell Biol 9:37
155. Nonhoff U, Ralser M, Welzel F et al (2007) Ataxin-2 interacts with the DEAD/H-box RNA helicase DDX6 and interferes with P-bodies and stress granules. Mol Biol Cell 18:1385–1396
156. Nishimoto Y, Ito D, Yagi T et al (2010) Characterization of alternative isoforms and inclusion body of the TAR DNA-binding protein-43. J Biol Chem 285:608–619
157. Bosco DA, Lemay N, Ko HK et al (2010) Mutant FUS proteins that cause amyotrophic lateral sclerosis incorporate into stress granules. Hum Mol Genet 19:4160–4175
158. Dormann D, Rodde R, Edbauer D et al (2010) ALS-associated fused in sarcoma (FUS) mutations disrupt Transportin-mediated nuclear import. EMBO J 29:2841–2857
159. Liu-Yesucevitz L, Bilgutay A, Zhang YJ et al (2010) Tar DNA binding protein-43 (TDP-43) associates with stress granules: analysis of cultured cells and pathological brain tissue. PLoS One 5:e13250

160. Nonaka T, Masuda-Suzukake M, Arai T et al (2013) Prion-like properties of pathological TDP-43 aggregates from diseased brains. Cell Rep 4:124–134
161. Couthouis J, Hart MP, Shorter J et al (2011) A yeast functional screen predicts new candidate ALS disease genes. Proc Natl Acad Sci USA 108:20881–20890
162. Couthouis J, Hart MP, Erion R et al (2012) Evaluating the role of the FUS/TLS-related gene EWSR1 in amyotrophic lateral sclerosis. Hum Mol Genet 21:2899–2911
163. Kim HJ, Kim NC, Wang YD et al (2013) Mutations in prion-like domains in hnRNPA2B1 and hnRNPA1 cause multisystem proteinopathy and ALS. Nature 495:467–473

RNP2 of RNA Recognition Motif 1 Plays a Central Role in the Aberrant Modification of TDP-43

Shinnosuke Takagi[1], Yohei Iguchi[1], Masahisa Katsuno[1]*, Shinsuke Ishigaki[1], Kensuke Ikenaka[1], Yusuke Fujioka[1], Daiyu Honda[1], Jun-ichi Niwa[2], Fumiaki Tanaka[3], Hirohisa Watanabe[1], Hiroaki Adachi[1], Gen Sobue[1]*

1 Department of Neurology, Nagoya University Graduate School of Medicine, Nagoya, Japan, **2** Stroke Center, Aichi Medical University, Aichi, Japan, **3** Department of Neurology and Stroke Medicine, Yokohama City University Graduate School of Medicine, Yokohama, Japan

Abstract

Phosphorylated and truncated TAR DNA-binding protein-43 (TDP-43) is a major component of ubiquitinated cytoplasmic inclusions in neuronal and glial cells of two TDP-43 proteinopathies, amyotrophic lateral sclerosis and frontotemporal lobar degeneration. Modifications of TDP-43 are thus considered to play an important role in the pathogenesis of TDP-43 proteinopathies. However, both the initial cause of these abnormal modifications and the TDP-43 region responsible for its aggregation remain uncertain. Here we report that the 32 kDa C-terminal fragment of TDP-43, which lacks the RNP2 motif of RNA binding motif 1 (RRM1), formed aggregates in cultured cells, and that similar phenotypes were obtained when the RNP2 motif was either deleted from or mutated in full-length TDP-43. These aggregations were ubiquitinated, phosphorylated and truncated, and sequestered the 25 kDa C-terminal TDP-43 fragment seen in the neurons of TDP-43 proteinopathy patients. In addition, incubation with RNase decreased the solubility of TDP-43 in cell lysates. These findings suggest that the RNP2 motif of RRM1 plays a substantial role in pathological TDP-43 modifications and that it is possible that disruption of RNA binding may underlie the process of TDP-43 aggregation.

Citation: Takagi S, Iguchi Y, Katsuno M, Ishigaki S, Ikenaka K, et al. (2013) RNP2 of RNA Recognition Motif 1 Plays a Central Role in the Aberrant Modification of TDP-43. PLoS ONE 8(6): e66966. doi:10.1371/journal.pone.0066966

Editor: Emanuele Buratti, International Centre for Genetic Engineering and Biotechnology, Italy

Received February 7, 2013; **Accepted** May 15, 2013; **Published** June 28, 2013

Funding: This work was supported by Center-of-Excellence (COE) grant; Ministry of Education, Culture, Sports, Science and Technology/Japan Society for the Promotion of Science KAKENHI Grant Numbers 21229011, 21689024, 22110005, and 23390230; Strategic Research Program for Brain Sciences, MEXT, Japan; Health Labour Sciences Research Grants, MHLW, Japan; and Core Research for Evolutional Science and Technology (CREST) of the Japan Science and Technology Agency (JST). The funders had no role in study design, data collection and analysis, decision to publish, or preparation of the manuscript.

Competing Interests: The authors have declared that no competing interests exist.

* E-mail: sobueg@med.nagoya-u.ac.jp (GS); ka2no@med.nagoya-u.ac.jp (MK)

Introduction

Amyotrophic lateral sclerosis (ALS) and certain forms of frontotemporal lobar degeneration (FTLD) with ubiquitin-positive but tau-negative inclusions have been considered to be a single disease spectrum of TAR DNA-binding protein 43 (TDP-43) proteinopathy since 2006, when this protein was reported to be a major component of ubiquitin-positive inclusions in the affected neuronal and glial cells of both ALS and FTLD [1–3]. The identification of missense mutations of *TARDBP*, the gene encoding TDP-43, in familial and sporadic ALS and/or FTLD patients further confirmed the importance of this molecule in the pathogenesis of TDP-43 proteinopathies [4–7].

Although TDP-43 normally localizes to the nucleus, it is distributed from nucleus to cytoplasm or neurite and forms aggregates that mainly consist of C-terminal fragments (CTFs) in the affected neurons of TDP-43 proteinopathy patients. In addition, aberrantly aggregated TDP-43 is hyperphosphorylated at multiple C-terminal sites [8]. The fact that most TDP-43 proteinopathy cases are sporadic suggests that exogenous factors induce the post-translational modifications of TDP-43 that are seen in the disease.

Although it does not fully recapitulate the pathological features of TDP-43 proteinopathies, artificial axonal damage induces transient cytoplasmic distribution of TDP-43 in mouse motor neurons [9,10], and several stress conditions, including oxidative stress and suppression of the ubiquitin-proteasome system, cause aberrant modifications of TDP-43 in cultured cell lines or primary neurons [11–15]. In addition, a motor neuron-specific disruption of proteasomes results in the cytosolic distribution of TDP-43 in a mouse model [16]. Finally, the repeat expansion of GGGGCC in C9orf72, as well as mutations in UBQLN2, VCP, PGRN, or OPTN, lead to neurodegeneration with TDP-43-positive neuronal inclusions [17–22].

These findings provide us with a clue for elucidating the mechanism of these modifications. Nevertheless, both the initial cause of these abnormal modifications and the region of TDP-43 responsible for its aggregation remain unknown. Here we report that RNP2 in RNA binding motif 1 (RRM1) plays a substantial role in the pathological TDP-43 modifications that are seen in TDP-43 proteinopathies.

Materials and Methods

Cell Culture and Treatment

Mouse NSC34 motor neuron-like cells (a kind gift of N.R. Cashman, University of British Columbia, Vancouver, Canada) [23] and human embryonic kidney 293 (HEK293) cells were

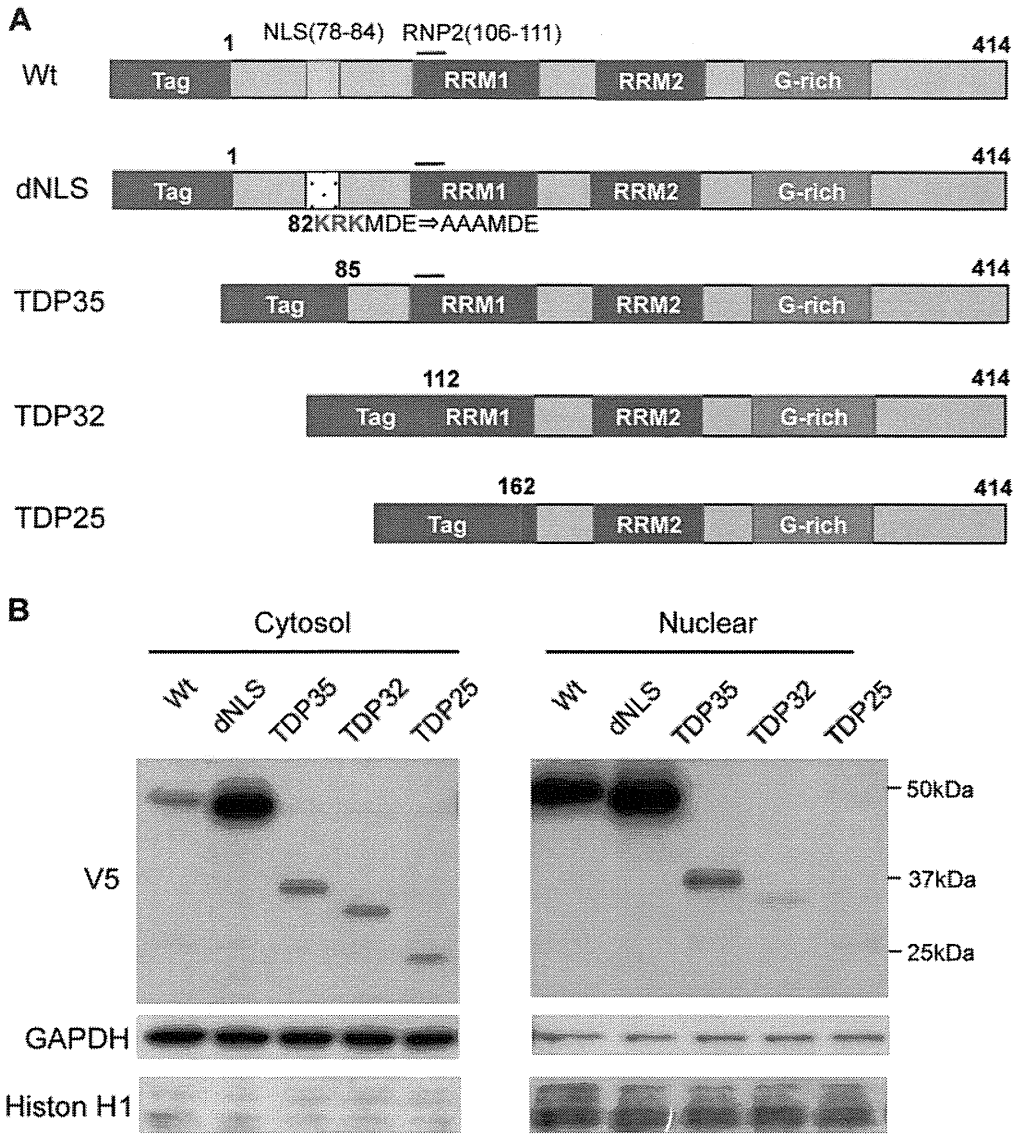

Figure 1. Intracellular localizations of TDP-43 lacking the NLS and of CTFs of TDP-43. (A) Structures of wild-type (Wt), NLS-disrupted mutant (dNLS) and CTFs (TDP35, TDP32 and TDP25). (B) Immunoblots of the cytosol and nuclear fractions from HEK293 cells expressing Wt, dNLS, TDP35, TDP32, or TDP25.
doi:10.1371/journal.pone.0066966.g001

cultured in a humidified atmosphere of 95% air/5% CO2 in a 37°C incubator in Dulbecco's Modified Eagle's Medium (DMEM) supplemented with 10% fetal bovine serum (FBS). In both NSC34 and HEK293 cells, the transfections of the intended plasmids were performed using Lipofectamine 2000 (Invitrogen), according to the manufacturer's instructions. Before performing subsequent experiments, the cells were incubated for 48 h after transfection.

DNA Constructs

Human wild-type TDP-43 (WT-TDP-43) (accession number NM 007375) cDNA was amplified by PCR from human spinal cord cDNA as previously described [11]. The PCR product was cloned into the pENTR/D-TOPO vector (Invitrogen). For the TDP-43 truncated fragments, amplified PCR products (for primers see Table S1) from the WT-TDP-43 vector were cloned into the pENTR/D-TOPO vector. For delta RNP2 TDP-43 (ΔRNP2), mutated RNP2 TDP-43 (mtRNP2), mutated RNP1 TDP-43 (mRNP1), delta RRM1 TDP-43 (ΔRRM1), and delta nuclear localization signal (NLS) TDP-43 (dNLS) vectors, primers containing mutant substitutions (Table S2) were used to mutagenize WT-TDP-43 (KOD-Plus-Mutagenesis kit; Toyobo). The entry vectors of each mutant TDP-43 vector were transferred into either a pcDNA6.2/N-EmGFP-DEST or pcDNA3.1/nV5-DEST vector using the Gateway LR Clonase II enzyme mix (Invitrogen). The sequences of all constructs were verified using the CEQ 8000 genetic analysis system (Beckman Coulter). The collection of autopsied human tissue and its use for this study were approved by the Ethics Committee of Nagoya University Graduate School of Medicine, and written informed consent was obtained from the patients' next-of-kin. The experimental procedure involving the human subject was conducted in conformance with the principles expressed in the Declaration of Helsinki.

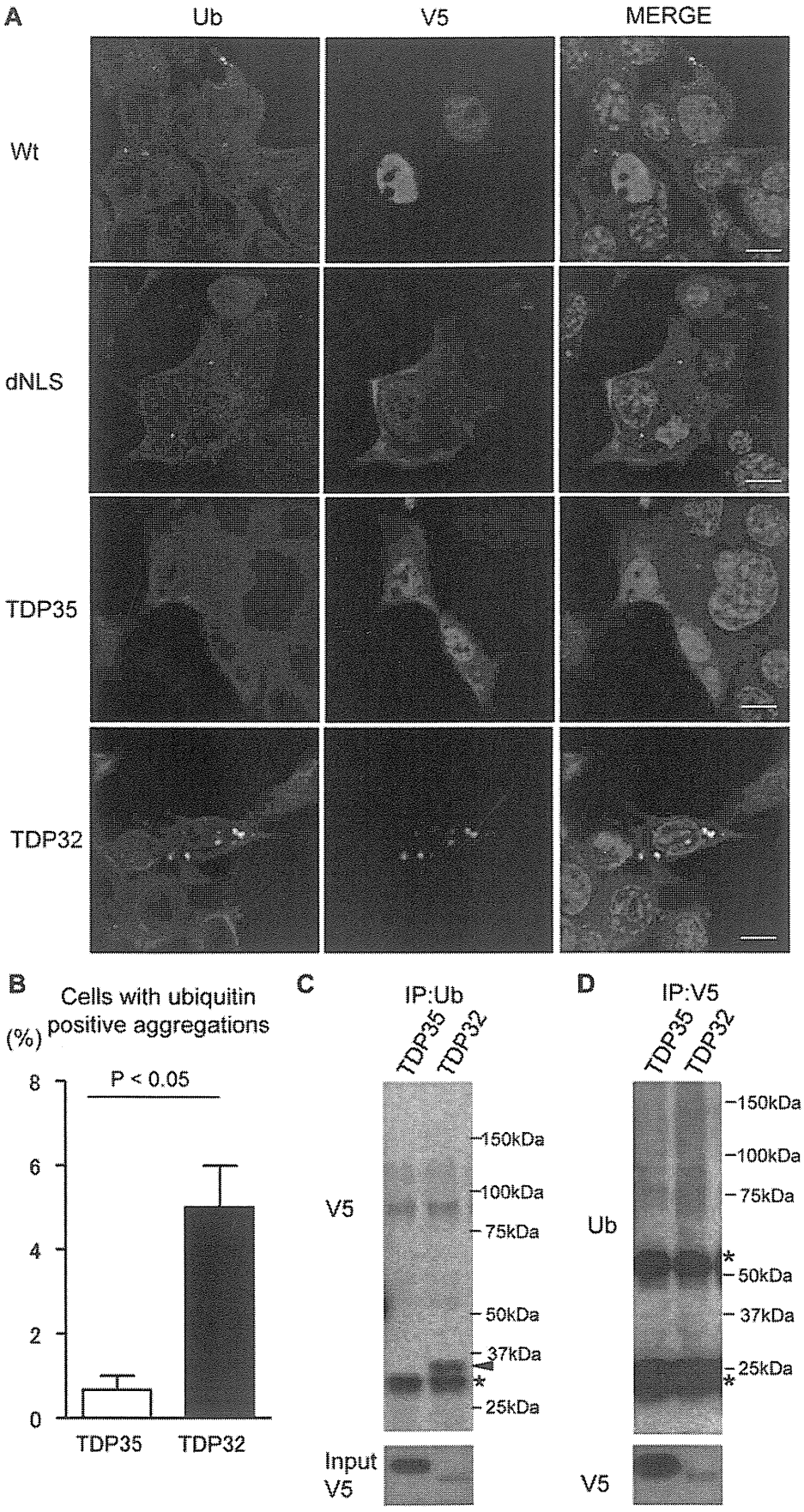
A
Ub
V5
MERGE
Wt
dNLS
TDP35
TDP32
B
Cells with ubiquitin positive aggregations
(%)
P < 0.05
8
6
4
2
0
TDP35
TDP32
C
IP:Ub
TDP35
TDP32
V5
150kDa
100kDa
75kDa
50kDa
37kDa
25kDa
Input V5
D
IP:V5
TDP35
TDP32
Ub
150kDa
100kDa
75kDa
50kDa
37kDa
25kDa
V5

Figure 2. Ubiquitination of TDP-43 CTFs. (A) Immunocytochemistry of NSC34 cells expressing Wt, dNLS, TDP35, or TDP32. Cells were stained with anti-ubiquitin antibody (green), anti-V5 antibody (red), and DAPI (blue). Scale bar = 5 μm. (B) Percentage of cells with ubiquitin-positive aggregates. Error bars indicate SEM (n = 3). The percentage of TDP32-expressing cells containing ubiquitin-positive aggregates was significantly higher than that of cells expressing TDP35 ($p<0.05$). (C) Immunoprecipitations with anti-ubiquitin antibody. The immunoreactivity of V5 was only detected in the TDP32 lane (arrow head). Asterisk indicates non-specific signal. (D) Immunoprecipitations with anti-V5 antibody. The ubiquitin-positive smear band was increased in the lane of TDP32 compared with that of TDP35. Asterisks indicate a heavy or light chain of IgG.
doi:10.1371/journal.pone.0066966.g002

Immunoblot Analysis

We used NE-PER Nuclear Cytoplasmic Reagents (Thermo Fisher Scientific) for the analysis of the cytoplasmic/nuclear ratio. For analysis of protein solubility, cells cultured in 10-cm plates were lysed in 1 ml RIPA buffer (Thermo Fisher Scientific). Lysates were sonicated and centrifuged at 100,000 *g* for 15 min. To prevent carryover, the pellets were washed with RIPA buffer, followed by sonication and centrifugation. RIPA-insoluble pellets were lysed in 100 μl urea buffer (7 M urea, 2 M thiourea, 4% CHAPS, 30 mM Tris, pH 8.5), sonicated, and centrifuged at 100,000 *g* for 15 min.

After the denaturation, 5 μl of each sample was separated by SDS-PAGE (5%–20% gradient gel) and the proteins were then transferred to Hybond-P membranes (Amersham Pharmacia Biotech). The membranes were blocked with 5% skimmed milk in Tris-buffered saline containing 0.05% Tween-20 and incubated with the intended primary antibodies. The primary antibodies used were as follows: anti-TDP-43 rabbit polyclonal antibody (1:1000; ProteinTech); anti-pTDP-43 (phospho Ser409/410) rabbit polyclonal antibody (1:1000; Cosmo Bio); anti-ubiquitin mouse monoclonal antibody (MBL); anti-histone H1 mouse monoclonal antibody (1:500; Millipore); anti-GAPDH mouse monoclonal antibody (1:2000; Temecula); anti-GFP mouse monoclonal antibody (1:2000; MBL); and anti-V5 mouse monoclonal antibody (1:5000; Invitrogen). For the anti-ubiquitin antibody, the membranes were fixed with 0.05% glutaraldehyde/0.1M KH_2PO_4 and blocked with 4% BSA. Secondary antibody probing and detection were performed using ECL Plus detection reagents (GE Healthcare). Chemiluminescence signals were digitized (LAS-3000 Imaging System; Fujifilm) and band intensities were quantified using Multi Gauge software (version 3.0; Fujifilm).

Immunocytochemistry

NSC34 cells were fixed in 4% paraformaldehyde, incubated in PBS containing 0.3% Triton X-100 for 5 min, blocked with Image-iT FX signal enhancer (Invitrogen), and incubated overnight at 4°C with anti-TDP-43 rabbit polyclonal antibody (1:1000; ProteinTech), anti-pTDP-43 (phospho Ser409/410) rabbit polyclonal antibody (1:500; Cosmo Bio), anti-TIAR mouse monoclonal antibody (1:500; BD Transduction Laboratories, Milan, Italy), anti-ubiquitin mouse monoclonal antibody (1:100; MBL), anti-V5 rabbit polyclonal antibody (1:1000; Bethyl) or anti-V5 mouse monoclonal antibody (Invitrogen). After washing, samples were incubated with Alexa-488-conjugated goat anti-mouse IgG and Alexa-555-conjugated goat anti-rabbit IgG (both at 1:1000; Invitrogen) for 60 min, mounted with Prolong Gold antifade reagent with DAPI (Invitrogen), and then imaged with a confocal microscope (LSM710; Zeiss).

For the counting of inclusion-bearing cells, we randomly selected 100 transfected cells from three separate experiments. The colocalization coefficient, which reflects the fraction of green pixels that are also positive for red pixels, was calculated using the Zeiss LSM software. We calculated the colocalization coefficient by randomly selected 10 fields from three separate experiments. To obtain images for calculating the colocalization coefficient, the settings of the confocal microscopy and the threshold of positive/negative fluorescence was fixed within each experiment.

Immunoprecipitation

Transfected HEK293 cells were washed with PBS and lysed in immunoprecipitation buffer (Thermo Fisher Scientific). After sonication on ice, the samples were agitated for 30 min at 4°C. The samples were centrifuged and supernatants were incubated with magnetic beads: anti-V5 magnetic beads (MBL), anti-GFP magnetic beads (MBL), and anti-ubiquitin magnetic beads (MBL). Samples were rotated overnight at 4°C. Immunoprecipitates were separated by SDS-PAGE (5%–20% gradient gel). Western blotting was performed using anti-V5-HRP antibody (MBL) and anti-GFP-HRP antibody (MBL).

Ribonucleoprotein Immunoprecipitation

Ribonucleoprotein (RNP) immunoprecipitation was performed using a RIP assay kit (MBL), according to the manufacturer's instructions. RNA concentrations were measured with a Nanodrop (Thermo Fisher Scientific). Electrophoresis of precipitated RNA was performed with a Bioanalyzer (Agilent Technologies) according to the manufacturer's instructions. For analysis of neurofilament light chain (hNFL) mRNA 3′UTR content, RNA obtained from immunoprecipitates was reverse transcribed into first-strand cDNA using SuperScript II reverse transcriptase (Invitrogen) and a PCR was performed with the following primers: ACCAACCAGTTGAGTTCCAGAT (forward) and GAATGATTCACATTGCCGTAGA (reverse).

Effect of RNase on TDP-43 Solubility

For analysis of protein solubility with or without RNase, HEK293 cells cultured in 10-cm plates were lysed in 1 ml of Tris-saline (TS) buffer (50 mM Tris-HCl buffer, pH 7.5, 0.15 M NaCl, 5 mM EDTA, protein phosphatase inhibitors, and a protease inhibitor cocktail). Lysates were sonicated and then divided into two samples. RNase A (10 μg/ml) was added to one of the samples. Samples incubated for 0 and 15 h at 4°C were centrifuged at 100,000 *g* for 15 min. To prevent carryover, the pellets were washed with TS buffer, followed by sonication and centrifugation. TS-insoluble pellets were lysed in 1 ml of Triton X-100 (TX) buffer (TS buffer containing 1% Triton X-100), sonicated, and centrifuged at 100,000 *g* for 15 min. The pellets were washed with TX buffer, followed by sonication and centrifugation. TX-insoluble pellets were lysed in 500 μl of Sarkosyl (Sar) buffer (TS buffer containing 1% Sarkosyl), sonicated and centrifuged at 100,000 *g* for 15 min. Sar-insoluble pellets were lysed in 100 μl of urea buffer.

Statistical Analyses

Statistical analyses were performed using GraphPad Prism software (GraphPad software inc.). Biochemical data were statistically analyzed using a Student's *t*-test or one-factor factorial ANOVA followed by Tukey post hoc tests. A p value of 0.05 or less was considered to be statistically significant.